AIMS Mathematics

http://www.aimspress.com/journal/Math

AIMS Mathematics, 10(12): 28829–28860.
DOI: 10.3934/math.20251269
Received: 18 September 2025
Revised: 10 November 2025
Accepted: 25 November 2025
Published: 09 December 2025

Research article

Hybrid inertial viscosity-type forward-backward splitting algorithms for variational inclusion problems

Doaa Filali[1], **Mohammad Dilshad**[2,*], **Mohammad Akram**[3,*], **Mohd. Falahat Khan**[4] **and Syed Shakaib Irfan**[4]

[1] Department of Mathematical Science, College of Sciences, Princess Nourah Bint Abdulrahman University, P.O. Box 84428, Riyadh 11671, Saudi Arabia
[2] Department of Mathematics, Faculty of Science, University of Tabuk, Tabuk-71491, Saudi Arabia
[3] Department of Mathematics, Faculty of Science, Islamic University of Madinah, Madinah 170, KSA
[4] Department of Mathematics, Aligarh Muslim University, Aligarh, 202002, U.P., India

* **Correspondence:** Email: mdilshaad@gmail.com, akramkhan_20@rediffmail.com.

Abstract: Herein, we aimed to develop two hybrid inertial viscosity-type forward-backward splitting algorithms for estimating the common solution of the variational inclusion problem and fixed point problem in Hilbert spaces. At the beginning of each iteration, the first algorithm estimated viscosity, fixed point, and inertial extrapolation. On the other hand, the second method estimated viscosity and inertial extrapolation alone. We demonstrated that the sequence induced by the proposed hybrid algorithms has strong convergence. We discussed a few special cases of the proposed algorithms and also presented theoretical applications of our findings. We furnished suitable numerical examples to validate the effectiveness of the recommended approaches.

Keywords: Hilbert space; inertial; viscosity approximation; variational inclusion; fixed point; convergence
Mathematics Subject Classification: 49J53, 49K99

1. Introduction

Throughout the work, we express the real Hilbert space by $\mathbb{H}$, and by $\mathbb{D} \neq \emptyset$ the close and convex subset of $\mathbb{H}$. The strong convergence of $\{w_k\}$ to w is symbolized by $w_k \to w$ and weak convergence by $w_k \rightharpoonup w$.

A significant problem of nonlinear analysis is the fixed point problem, which offers a logical and cohesive framework for studying a broader class of problems, including finance, network analysis, and optimization, for instance, see [13, 35, 39, 41] and their references. The fixed point problem (FPP) for a nonexpansive mapping $S : \mathbb{H} \to \mathbb{H}$ is as follows:

$$\text{Determine } \tilde{o} \in \mathbb{H} \text{ so that } S(\tilde{o}) = \tilde{o}.$$

In the past few years, numerous approaches have been carried out to deal with the FPP. Mann's iterative technique [28] is the main source of motivation for most of the schemes used to approximate the fixed point, namely, for $w_0 \in \mathbb{D}$, compute

$$w_{k+1} = \psi_k w_k + (1 - \psi_k) S w_k, \quad k \geq 0,$$

where $S : \mathbb{D} \to \mathbb{D}$ is nonexpansive and ψ_k is a controlling parameter, which forces the sequence $\{w_k\} \rightharpoonup \tilde{o}$, where $\tilde{o}$ is a fixed point of S. Moudafi [27] suggested the viscosity approximation method by adding S with a contraction Q. For any $w_0 \in \mathbb{D}$ and $\psi_k \in (0, 1)$, compute w_k generated by

$$w_{k+1} = \psi_k Q(w_k) + (1 - \psi_k) S w_k, \quad k \geq 0.$$

The sequence $w_k \to \tilde{o}$, where $\tilde{o}$ belongs to the fixed point set of S.

Another important problem in nonlinear analysis is the variational inclusion problem ($\text{VI}_{\text{nclusion}}\text{P}$), for the monotone mappings $B : \mathbb{H} \to \mathbb{H}$ and $G : \mathbb{H} \to 2^{\mathbb{H}}$, that is:

$$\text{Determine } \tilde{o} \in \mathbb{H} \text{ so that } 0 \in (B + G)\tilde{o}.$$

Numerous key ideas of applied mathematics, such as minimization, equilibrium, variational inequality, saddle point, and split feasibility problems, are based on the study of $\text{VI}_{\text{nclusion}}\text{P}$. Moreover, it represents many problems of applied sciences including image reconstruction, signal processing, machine learning and optimal control; see [3, 4, 12, 18, 20, 22, 23, 29, 38] and the references inside. Due to its application oriented nature, many researchers have studied $\text{VI}_{\text{nclusion}}\text{P}$ and suggested various iterative algorithms for solving $\text{VI}_{\text{nclusion}}\text{P}$.

Lions and Mercier [22] investigated the forward-backward splitting algorithm for $\text{VI}_{\text{nclusion}}\text{P}$:

$$w_{k+1} = R^G_{\mu_k}(I - \mu_k B) w_k, \quad k \geq 0,$$

where $\mu_k > 0$, $(I - \mu_k B)$ is termed as the forward operator and $R^G_{\mu_k} = (I + \mu_k G)^{-1}$ is called the resolvent of operator G referred to as the backward operator. They also proved the weak convergence theorem. In the recent past, the forward-backward technique has been studied, altered, and extended by numerous researchers; see [7, 16, 21, 23, 31, 33, 38] and the references therein.

If $B = 0$, we obtain the following monotone inclusion problem (MIP):

$$\text{Determine } \tilde{o} \in \mathbb{H} \text{ so that } 0 \in G(\tilde{o}).$$

Alvarez and Attouch [5] suggested a new technique to estimate the solution of the MIP, which is given by:

$$w_{k+1} = R^G_{\mu}[w_k + \sigma_k(w_k - w_{k-1})],$$

and the weak convergence of $\{w_k\}$ has been studied under the following assumption:

$$\sum_{k=1}^{\infty} \sigma_k \|w_k - w_{k-1}\|^2 < +\infty.$$

This technique is known as an inertial proximal point method, and the expression $\sigma_k(w_k - w_{k-1})$ is called inertial extrapolation. It is noted that due to its design, the sequence obtained from the inertial proximal point method converges quickly. Therefore, the inertial term has a key role to accelerate the convergence; hence, adopted by a number of authors, see [11, 14, 15, 17, 26] and references therein.

In [26], Moudafi and Oliny suggested the inertial proximal point technique to solve $\mathrm{VI_{nclusion}P}$:

$$\begin{cases} u_k = w_k + \sigma_k(w_k - w_{k-1}), \\ w_{k+1} = [I + \mu_k G]^{-1}(u_k - \mu_k B w_k), \end{cases}$$

where $\mu_k \in (0, 2/\kappa)$, and B is κ-Lipschitz continuous. They established the weak convergence of $\{w_k\}$ using the same restriction as in [5]. Lorenz and Pock [21] proposed the following modified version of [26] and proved the weak convergence of $\{w_k\}$ to the solution of ($\mathrm{VI_{nclusion}P}$):

$$\begin{cases} u_k = w_k + \sigma_k(w_k - w_{k-1}), \\ w_{k+1} = [I + \mu_k G]^{-1}(I - \mu_k B) u_k, \end{cases}$$

where μ_k is a step-size parameter and $\sigma \in [0, 1)$. Recently, the $\mathrm{VI_{nclusion}P}$ and FPP were explored by Thong et al. [37]. They suggested the inertial viscosity method, for finding the common solutions:

Algorithm 1.1. (Algorithm 3 of [37]) Select w_0 and w_1 and assign $k = 1$.
Step 1. Compute

$$\begin{aligned} u_k &= w_k + \sigma_k(w_k - w_{k-1}), \\ v_k &= [I + \mu G]^{-1}(I - \mu B) u_k. \end{aligned}$$

If $u_k = v_k$, then stop. Or else, go to Step 2.
Step 2. Compute

$$w_{k+1} = \psi_k Q(w_k) + (1 - \psi_k) S v_k.$$

Assign $k = k+1$ and go back to Step 1, where G is a maximal monotone, B is κ-ism, S is a nonexpansive, Q is a contraction, and $\mu \in (0, 2\kappa)$. They studied the strong convergence of $\{w_k\}$ using the following assumptions on parameters:

(i) $\psi_k \in (0, 1),\ \lim_{k\to\infty} \psi_k = 0,\ \sum_{k=1}^{\infty} \psi_k = \infty,\ \lim_{k\to\infty} \frac{\psi_{k-1}}{\psi_k} = 1,$
(ii) $\sigma_k \in [0, \sigma), \sigma > 0,\ \lim_{k\to\infty} \frac{\sigma_k}{\psi_k} \|w_k - w_{k-1}\| = 0.$

Recently, Reich and Taiwo [32] have looked into the hybrid viscosity-type iterative methods to deal with the solution of the variational inclusion problem. Tang et al. [40] presented some inertial methods and studied their convergence analysis for solving variational inclusion problems. Numerous iterative methods for exploring the common solution can also be seen in [1,2,9–11,14,15] and references inside.

Following the above discussed excellent work, we develop two hybrid inertial viscosity-type forward-backward splitting iterative algorithms for solving $VI_{nclusion}P$ and FPP in which we compute the viscosity, fixed point and inertial term all together in the beginning of each step. We present two special cases of our iterative algorithms. Some theoretical applications are also obtained from the proposed algorithms. Examples in finite and infinite dimensional Hilbert spaces are used to examine and for comparing the suggested iterative techniques with Algorithm 3 of [37].

2. Preliminaries

For all ϱ, ϑ, η in Hilbert space $\mathbb{H}$, $m_1, m_2, m_3 \in [0,1]$ such that $m_1 + m_2 + m_3 = 1$, the following equality and inequality hold in Hilbert space $\mathbb{H}$:

$$\begin{aligned} \|m_1\varrho + m_2\vartheta + m_3\eta\|^2 &= m_1\|\varrho\|^2 + m_2\|\vartheta\|^2 + m_3\|\eta\|^2 \\ &\quad -m_1m_2\|\varrho - \vartheta\|^2 - m_2m_3\|\vartheta - \eta\|^2 - m_3m_1\|\eta - \varrho\|^2 \end{aligned} \tag{2.1}$$

and

$$\|\varrho \pm \vartheta\|^2 = \|\varrho\|^2 \pm 2\langle\varrho, \vartheta\rangle + \|\vartheta\|^2 \leq \|\varrho\|^2 \pm 2\langle\vartheta, \varrho + \vartheta\rangle. \tag{2.2}$$

Definition 2.1. [6] A mapping $S : \mathbb{H} \to \mathbb{H}$ is called

(a) averaged, if $S = (1-\alpha)I + \alpha f, \forall \alpha \in (0,1)$, where $f : \mathbb{H} \to \mathbb{H}$ is a nonexpansive mapping.
(b) η-Lipschitzian, if $\|S(\varrho) - S(\vartheta)\| \leq \eta\|\varrho - \vartheta\|,\ \forall\, \varrho, \vartheta \in \mathbb{H}, \eta > 0$;
(c) contraction, if $\|S(\varrho) - S(\vartheta)\| \leq \theta\|\varrho - \vartheta\|,\ \forall\, \varrho, \vartheta \in \mathbb{H}, \theta \in (0,1)$;
(d) nonexpansive, if $\|S(\varrho) - S(\vartheta)\| \leq \|\varrho - \vartheta\|, \forall\, \varrho, \vartheta \in \mathbb{H}$;
(e) firmly nonexpansive, if $\|S(\varrho) - S(\vartheta)\|^2 \leq \langle\varrho - \vartheta, S(\varrho) - S(\vartheta)\rangle, \forall\, \varrho, \vartheta \in \mathbb{H}$;
(f) κ-inverse strongly monotone (κ-ism), if $\exists\, \kappa > 0$ so that

$$\langle S(\varrho) - S(\vartheta), \varrho - \vartheta\rangle \geq \kappa\|S(\varrho) - S(\vartheta)\|^2, \forall\, \varrho, \vartheta \in \mathbb{H};$$

(g) monotone, if

$$\langle S(\varrho) - S(\vartheta), \varrho - \vartheta\rangle \geq 0, \forall\, \varrho, \vartheta \in \mathbb{H}.$$

Definition 2.2. [8] A set-valued mapping $G : \mathbb{H} \to 2^{\mathbb{H}}$ is called

(a) monotone, if $\langle\eta - \zeta, \varrho - \vartheta\rangle \geq 0, \forall \eta, \zeta, \in \mathbb{H}, \varrho \in G(\eta), \vartheta \in G(\zeta)$;
(b) $Graph(G) = \{(\eta, \zeta) \in \mathbb{H} \times \mathbb{H} : \zeta \in G(\eta)\}$;
(c) maximal monotone, if G is monotone and $(I + \mu G)(\mathbb{H}) = \mathbb{H}, \mu > 0$.

The resolvent of G is defined by $R_\mu^G = [I + \mu G]^{-1}, \mu > 0$, where I is the identity operator.

Definition 2.3. [8] The metric projection of $\mathbb{H}$ onto $\mathbb{D}$ is a mapping which assigns each value point $\eta \in \mathbb{H}$ to a unique nearest point in $\mathbb{D}$, that is

$$\|\eta - P_{\mathbb{D}}\eta\| \leq \|\eta - \zeta\|, \forall\, \zeta \in \mathbb{D}. \tag{2.3}$$

Some properties of $P_{\mathbb{D}}$ are summarized as follows:

$$\langle \varrho - \vartheta, \quad P_{\mathbb{D}}\varrho - P_{\mathbb{D}}\vartheta \rangle \geq \|P_{\mathbb{D}}\varrho - P_{\mathbb{D}}\vartheta\|^2, \quad \varrho, \vartheta \in \mathbb{H},$$

and

$$\langle \varrho - P_{\mathbb{D}}\varrho, \quad \vartheta - P_{\mathbb{D}}\varrho \rangle \leq 0, \quad \forall \varrho \in \mathbb{H}, \vartheta \in \mathbb{D}.$$

Remark 2.1. (a) Note that κ-ism mapping is monotone and $\frac{1}{\kappa}$-Lipschitzian.
(b) Every averaged mapping is nonexpansive but the converse need not be true in general.
(c) S is firmly nonexpansive if, and only if, $I - S$ is firmly nonexpansive.
(d) If f and g are averaged, then $f \circ g$ is averaged.

Remark 2.2. (a) If G is a maximal monotone mapping, then R_μ^G is single-valued, nonexpansive and firmly nonexpansive.
(b) R_μ^G is firmly nonexpansive if, and only if,

$$\|R_\mu^G \varrho - R_\mu^G \vartheta\|^2 \leq \|\varrho - \vartheta\|^2 - \|(I - R_\mu^G)\varrho - (I - R_\mu^G)\vartheta\|^2, \text{ for all } \varrho, \vartheta \in \mathbb{H}.$$

(c) The operator $I - R_\mu^G$ is nonexpansive and so it is demiclosed at zero.
(d) w solves ($\mathrm{VI_{nclusion}P}$) $\Leftrightarrow w = R_\mu^G(I - \mu B)w$.

Lemma 2.1. *[42] Suppose that $Q : \mathbb{H} \to \mathbb{H}$ is θ-Lipschitz continuous and κ-strongly monotone over a closed and convex subset $\mathbb{D} \subset \mathbb{H}$. Then, the variational inequality problem*

$$\text{find } \tilde{o} \in \mathbb{D} \text{ such that } \langle Q(\tilde{o}), w - \tilde{o} \rangle \geq 0, \ \forall\, w \in \mathbb{D}$$

has a unique solution $\tilde{o} \in \mathbb{D}$.

Remark 2.3. It can be easily verified that for a nonempty closed convex subset $\mathbb{D}$ of $\mathbb{H}$, the following are equivalent

(a) find $\tilde{o} \in \mathbb{D}$ such that $P_{\mathbb{D}}Q(\tilde{o}) = \tilde{o}$;
(b) find $\tilde{o} \in \mathbb{D}$ such that $\langle (I - Q)(\tilde{o}), w - \tilde{o} \rangle \geq 0, \ \forall\, w \in \mathbb{D}$, where I is the identity operator.

Lemma 2.2. *[19] Suppose $\emptyset \neq \mathbb{D} \subseteq \mathbb{H}$ and $S : \mathbb{D} \to \mathbb{D}$ is a nonexpansive mapping with the properties*

(a) $\mathrm{Fix}(S) \neq \emptyset$,
(b) the sequence $\{w_k\} \rightharpoonup \tilde{o}$ and $\lim_{k\to\infty} \|S w_k - w_k\| = 0$.

Then, $S\tilde{o} = \tilde{o}$.

Lemma 2.3. *[41] If $\{w_k\}$ is a sequence of nonnegative real numbers for which*

$$w_{k+1} \leq (1 - \psi_k)w_k + \psi_k \varphi_k, \quad k \geq 0,$$

where $\{\psi_k\} \in (0, 1)$ and $\{\varphi_k\}$ is a sequence of real numbers satisfying

(a) $\lim_{k\to\infty} \psi_k = 0$, and $\sum_{k=1}^{\infty} \psi_k = \infty$,

(b) $\limsup_{k\to\infty} \varphi_k \leq 0.$

Then, $\lim_{k\to\infty} w_k = 0.$

Lemma 2.4. *[30] Let* $\{w_k\}$ *be a sequence in Hilbert space* $\mathbb{H}$ *for which a closed and convex subset* $\mathbb{D} \neq \emptyset$ *of* $\mathbb{H}$ *exists such that*

(a) $\lim_{k\to\infty} \|w_k - w\|$ *exists for every* $w \in \mathbb{D}$*,*
(b) any weak cluster point of $\{w_k\}$ *falls within* $\mathbb{D}$*.*

Then there exists $w^\star \in \mathbb{D}$ *satisfying* $w_k \rightharpoonup w^\star$*.*

Lemma 2.5. *[24] Let* $\{w_k\}$ *be a sequence of real numbers that does not decrease at infinity in the sense that one can find a subsequence* $\{w_{k_m}\}$ *of* $\{w_k\}$ *satisfying* $w_{k_m} < w_{k_m+1}$ *for all* $m \geq 0$*. Also consider the sequence of integers* $\{\Im(k)\}_{k\geq k_0}$ *defined by*

$$\Im(k) = \max\{m \leq k : w_k \leq w_{k+1}\}.$$

Then $\{\Im(k)\}_{k\geq k_0}$ *is a nondecreasing sequence verifying* $\lim_{k\to\infty} \Im(k) = \infty$ *and* $\forall\, k \geq k_0$*,*

$$\max\{w_{\Im(k)}, w_{(k)}\} \leq w_{\Im(k)+1}.$$

3. Main contribution

The solution sets of $\mathrm{VI_{nclusion}P}$ and FPP are indicated by Φ and Ω, correspondingly. To ensure the convergence of the proposed methods, we consider assumptions listed below:
($\mathbf{A_1}$) $B : \mathbb{H} \to \mathbb{H}$ such that B is a κ-inverse strongly monotone operator;
($\mathbf{A_2}$) $G : \mathbb{H} \to 2^{\mathbb{H}}$ is a maximal monotone operator;
($\mathbf{A_3}$) $S : \mathbb{H} \to \mathbb{H}$ is nonexpansive and $Q : \mathbb{H} \to \mathbb{H}$ is θ-contraction;
($\mathbf{A_4}$) $\psi_k \in (0,1)$ so that $\lim_{k\to\infty} \psi_k = 0$, $\sum_{k=1}^{\infty} |\psi_k - \psi_{k-1}| < \infty$ and $\sum_{k=1}^{\infty} \psi_k = \infty$;
($\mathbf{A_5}$) $\{\tau_k\}$ is a positive sequence such that $\sum_{n=1}^{\infty} \tau_k < \infty$ and $\lim_{k\to\infty} \frac{\tau_k}{\psi_k} = 0$;
($\mathbf{A_6}$) The common solution set of $\mathrm{VI_{nclusion}P}$ and FPP is expressed by $\Phi \cap \Omega$ and $\Phi \cap \Omega \neq \emptyset$.

Algorithm 3.1. Hybrid inertial iterative method 1

Choose $\sigma \in [0,1)$, and $0 < \mu < \mu_k < 2\kappa$ is given. Pick the initial points w_0 and w_1.
Iterative Step: For $k \geq 1$ and iterates w_k, w_{k-1}, select $0 < \sigma_k < \overline{\sigma}_k$, where

$$\overline{\sigma}_k = \begin{cases} \min\{\frac{\tau_k}{\|w_k - w_{k-1}\|}, \quad \sigma\}, & \text{if } w_k \neq w_{k-1}, \\ \sigma, & \text{otherwise.} \end{cases} \tag{3.1}$$

Compute

$$u_k = \psi_k Q(w_k) + (1-\psi_k)[S(w_k) + \sigma_k(w_k - w_{k-1})], \tag{3.2}$$

$$v_k = R^G_{\mu_k}(u_k - \mu_k B u_k) \tag{3.3}$$

$$w_{k+1} = R^G_{\mu_k}(v_k - \mu_k B v_k) \tag{3.4}$$

If $w_{k+1} = v_k = w_k = u_k$, then exit, or else, assign $k = k+1$ and back to the computation.

Remark 3.1. If $w_{k+1} = w_k = v_k = u_k$ in Algorithm 3.1, we get

$$w_k = R^G_{\mu_k}(w_k - \mu_k B w_k) = (I + \mu_k G)^{-1}(w_k - \mu_k B w_k)$$

which implies that $w_k \in (B+G)^{-1}(0)$, that is, $w_k \in \Phi$. Furthermore, from (3.2), we also have $w_{k+1} = \psi_k Q(w_k) + (1-\psi_k)S(w_k)$, which is the viscosity approximation method [27], hence, $\{w_k\}$ converges to some point in Ω.

Remark 3.2. From (3.1), we have that $\lim\limits_{k\to\infty} \frac{\sigma_k\|w_k - w_{k-1}\|}{\psi_k} = 0$, and joining with $\lim\limits_{k\to\infty} \frac{\tau_k}{\psi_k} = 0$, we obtain

$$\lim_{k\to\infty} \frac{\sigma_k\|w_k - w_{k-1}\|}{\psi_k} \leq \lim_{k\to\infty} \frac{\tau_k}{\psi_k} = 0.$$

Hence there exists a constant L_1 such that $\frac{\sigma_k\|w_k - w_{k-1}\|}{\psi_k} \leq L_1$ or $\sigma_k\|w_k - w_{k-1}\| \leq L_1\psi_k$.

Theorem 3.1. *If the assumptions $(A_1)-(A_6)$ hold, suppose $\{w_k\}$ induced by Algorithm 3.1, then $w_k \to w$ such that $w = P_{\Phi\cap\Omega}Q(w)$.*

Proof For a θ-contraction mapping Q, it is easy to see that $(I - Q)$ is $(1+\theta)$-Lipschitz continuous and $(1-\theta)$-strongly monotone (see [36]). Hence, Lemma 2.1 ensured the existence of unique $\tilde{o} \in \Phi\cap\Omega$ such that $\tilde{o} = P_{\Phi\cap\Omega}Q(\tilde{o})$. It is given that B is κ-ism. Then, in view of Remark 2.2(2) and 2.2(3), we have

$$\begin{aligned} & \|v_k - \tilde{o}\|^2 = \|R^G_{\mu_k}(u_k - \mu_k B u_k) - \tilde{o}\|^2 \\ \leq\ & \|u_k - \mu_k B u_k - \tilde{o} + \mu_k B\tilde{o}\|^2 - \|(I - R^G_{\mu_k})(u_k - \mu_k B u_k) \\ & -(I - R^G_{\mu_k})(\tilde{o} - \mu_k B\tilde{o})\|^2 \\ =\ & \|u_k - \tilde{o} - \mu_k(Bu_k - B\tilde{o})\|^2 - \|u_k - v_k - \mu_k(Bu_k - B\tilde{o})\|^2 \\ \leq\ & \|u_k - \tilde{o}\|^2 - 2\mu_k\langle Bu_k - B\tilde{o}, u_k - \tilde{o}\rangle - \|u_k - v_k\|^2 + 2\mu_k\langle Bu_k - B\tilde{o}, u_k - v_k\rangle \\ \leq\ & \|u_k - \tilde{o}\|^2 - 2\mu_k\kappa\|Bu_k - B\tilde{o}\|^2 - \|u_k - v_k\|^2 + 2\mu_k\langle Bu_k - B\tilde{o}, u_k - v_k\rangle. \end{aligned} \tag{3.5}$$

Furthermore, we have

$$\left\|Bu_k - B\tilde{o} - \frac{u_k - v_k}{2\kappa}\right\|^2 = \|Bu_k - B\tilde{o}\|^2 + \left\|\frac{u_k - v_k}{2\kappa}\right\|^2 - \frac{1}{\kappa}\left\langle Bu_k - B\tilde{o}, u_k - v_k\right\rangle$$

or

$$\begin{aligned} -2\mu_k\kappa\|Bu_k - B\tilde{o}\|^2 + 2\mu_k\left\langle Bu_k - B\tilde{o}, u_k - v_k\right\rangle &= -2\mu_k\kappa\left\|Bu_k - B\tilde{o} - \frac{u_k - v_k}{2\kappa}\right\|^2 \\ &\quad +2\mu_k\kappa\left\|\frac{u_k - v_k}{2\kappa}\right\|^2. \end{aligned} \tag{3.6}$$

By using (3.5) and (3.6), we get

$$\begin{aligned} \|v_k - \tilde{o}\|^2 &\leq \|u_k - \tilde{o}\|^2 - 2\mu_k\kappa\left\|Bu_k - B\tilde{o} - \frac{u_k - v_k}{2\kappa}\right\|^2 - (\frac{2\kappa - \mu_k}{2\kappa})\|u_k - v_k\|^2 & (3.7)\\ &\leq \|u_k - \tilde{o}\|^2. & (3.8) \end{aligned}$$

Since $R^G_{\mu_k}(I - \mu_k B)$ is averaged, hence, nonexpansive (see [25]), from (3.4) and (3.6), it follows that

$$\begin{aligned} \|w_{k+1} - \tilde{o}\|^2 &= \|R^G_{\mu_k}(v_k - \mu_k Bv_k) - \tilde{o}\|^2 \\ &= \|R^G_{\mu_k}(I - \mu_k B)v_k - R^G_{\mu_k}(I - \mu_k B)\tilde{o}\|^2 \\ &\leq \|v_k - \tilde{o}\|^2 & (3.9)\\ &\leq \|u_k - \tilde{o}\|^2 - 2\mu_k\kappa\left\|Bu_k - B\tilde{o} - \frac{u_k - v_k}{2\kappa}\right\|^2 \\ &\quad -(\frac{2\kappa - \mu_k}{2\kappa})\|u_k - v_k\|^2. & (3.10) \end{aligned}$$

From Remark 2.2, $\sigma_k\|w_k - w_{k-1}\| \leq \psi_k L_1$, for some constant $L_1 > 0$. Since h is θ-contraction, using (3.2), (3.8), (3.9) and applying mathematical induction, we have

$$\begin{aligned} \|u_k - \tilde{o}\| &= \|\psi_k Q(w_k) + (1 - \psi_k)[S(w_k) + \sigma_k(w_k - w_{k-1})] - \tilde{o}\| \\ &= \psi_k\|Q(w_k) - \tilde{o}\| + (1 - \psi_k)\|S(w_k) - \tilde{o} + \sigma_k(w_k - w_{k-1})\| \\ &\leq \psi_k\|Q(w_k) - Q(\tilde{o})\| + \psi_k\|Q(\tilde{o}) - \tilde{o}\| + (1 - \psi_k)[\|S(w_k) - \tilde{o}\| \\ &\quad +\sigma_k\|(w_k - w_{k-1})\|] \\ &\leq \psi_k\theta\|w_k - \tilde{o}\| + \psi_k\|Q(\tilde{o}) - \tilde{o}\| + (1 - \psi_k)\|w_k - \tilde{o}\| + \psi_k L_1 \\ &= [1 - \psi_k(1 - \theta)]\|w_k - \tilde{o}\| + \psi_k(1 - \theta)\frac{\|Q(\tilde{o}) - \tilde{o}\| + L_1}{1 - \theta} \\ &\leq \max\left\{\|w_k - \tilde{o}\|, \quad \frac{\|Q(\tilde{o}) - \tilde{o}\| + L_1}{1 - \theta}\right\} \\ &\leq \max\left\{\|v_{k-1} - \tilde{o}\|, \quad \frac{\|Q(\tilde{o}) - \tilde{o}\| + L_1}{1 - \theta}\right\} \\ &\leq \max\left\{\|u_{k-1} - \tilde{o}\|, \quad \frac{\|Q(\tilde{o}) - \tilde{o}\| + L_1}{1 - \theta}\right\} \\ &\vdots \\ &\leq \max\left\{\|u_0 - \tilde{o}\|, \quad \frac{\|Q(\tilde{o}) - \tilde{o}\| + L_1}{1 - \theta}\right\}, \end{aligned}$$

which suggests that $\{u_k\}$ is bounded and, hence, $\{w_k\}$ and $\{v_k\}$ are as well. Let $x_k = S(w_k)+\sigma_k(w_k-w_{k-1})$. Note that $\{x_k\}$ is also bounded. By using (3.2), first we estimate

$$\begin{aligned}\|x_k - \tilde{o}\|^2 &= \|S(w_k) + \sigma_k(w_k - w_{k-1}) - \tilde{o}\|^2 \\ &= \|S(w_k) - \tilde{o}\|^2 + 2\sigma_k\langle w_k - w_{k-1}, x_k - \tilde{o}\rangle \\ &\leq \|S(w_k) - \tilde{o}\|^2 + 2\sigma_k\|w_k - w_{k-1}\|\|x_k - \tilde{o}\| \\ &\leq \|w_k - \tilde{o}\|^2 + 2d_k\|x_k - \tilde{o}\|, \end{aligned} \tag{3.11}$$

where $d_k = \sigma_k\|w_k - w_{k-1}\|$, and

$$\begin{aligned}\langle Q(w_k) - \tilde{o}, x_k - \tilde{o}\rangle &= \langle Q(w_k) - Q(\tilde{o}), x_k - \tilde{o}\rangle + \langle Q(\tilde{o}) - \tilde{o}, x_k - \tilde{o}\rangle \\ &\leq \|Q(w_k) - Q(\tilde{o})\|\|x_k - \tilde{o}\| + \langle Q(\tilde{o}) - \tilde{o}, x_k - \tilde{o}\rangle \\ &\leq \frac{1}{2}\{\theta^2\|w_k - \tilde{o}\|^2 + \|x_k - \tilde{o}\|^2\} \\ &\quad +\langle Q(\tilde{o}) - \tilde{o},\ \ x_k - \tilde{o}\rangle, \end{aligned} \tag{3.12}$$

and

$$\begin{aligned}&\langle Q(\tilde{o}) - \tilde{o},\ \ x_k - \tilde{o}\rangle = \langle Q(\tilde{o}) - \tilde{o},\ \ S(w_k) + \sigma_k(w_k - w_{k-1}) - \tilde{o}\rangle \\ \leq\ & \langle Q(\tilde{o}) - \tilde{o},\ \ S(w_k) - \tilde{o}\rangle + \langle Q(\tilde{o}) - \tilde{o},\ \ \sigma_k(w_k - w_{k-1})\rangle \\ \leq\ & \langle Q(\tilde{o}) - \tilde{o},\ \ S(w_k) - \tilde{o}\rangle + \|Q(\tilde{o}) - \tilde{o}\|\sigma_k\|w_k - w_{k-1}\| \\ \leq\ & \langle Q(\tilde{o}) - \tilde{o},\ \ S(w_k) - \tilde{o}\rangle + d_k\|Q(\tilde{o}) - \tilde{o}\|. \end{aligned} \tag{3.13}$$

By using (3.11)–(3.13), we obtain

$$\begin{aligned}\|u_k - \tilde{o}\|^2 &= \|\psi_k Q(w_k) + (1-\psi_k)x_k - \tilde{o}\|^2 \\ &= \psi_k^2\|Q(w_k) - \tilde{o}\|^2 + (1-\psi_k)^2\|x_k - \tilde{o}\|^2 + 2\psi_k(1-\psi_k)\langle Q(w_k) - \tilde{o}, x_k - \tilde{o}\rangle \\ &\leq \psi_k^2\|Q(w_k) - \tilde{o}\|^2 + (1-\psi_k)^2\|x_k - \tilde{o}\|^2 + \psi_k(1-\psi_k)[\theta^2\|w_k - \tilde{o}\|^2 \\ &\quad +\|x_k - \tilde{o}\|^2] + d_k\|Q(\tilde{o}) - \tilde{o}\| + 2\psi_k(1-\psi_k)\langle Q(\tilde{o}) - \tilde{o},\ \ S(w_k) - \tilde{o}\rangle \\ &\leq (1-\psi_k)\|x_k - \tilde{o}\|^2 + \psi_k\theta^2\|w_k - \tilde{o}\|^2 \\ &\quad +\psi_k\Big\{\psi_k\|Q(w_k) - \tilde{o}\|^2 + 2(1-\psi_k)\langle Q(\tilde{o}) - \tilde{o},\ \ S(w_k) - \tilde{o}\rangle\Big\} \\ &\leq [1 - \psi_k(1-\theta^2)]\|w_k - \tilde{o}\|^2 + \psi_k\Big\{\psi_k\|Q(w_k) - \tilde{o}\|^2 \\ &\quad +2(1-\psi_k)\langle Q(\tilde{o}) - \tilde{o},\ \ S(w_k) - \tilde{o}\rangle + d_k\|Q(\tilde{o}) - \tilde{o}\| + \frac{2d_k}{\psi_k}\|x_k - \tilde{o}\|\Big\} \end{aligned} \tag{3.14}$$

Let $\gamma_k = \psi_k(1-\theta^2)$. Then, it follows from (3.10) and (3.14) that

$$\begin{aligned}\|w_{k+1} - \tilde{o}\|^2 &\leq (1-\gamma_k)\|w_k - \tilde{o}\|^2 - 2\mu_k\kappa\Big\|Bu_k - B\tilde{o} - \frac{u_k - v_k}{2\kappa}\Big\|^2 \\ &\quad -\Big(\frac{2\kappa - \mu_k}{2\kappa}\Big)\|u_k - v_k\|^2 + \gamma_k E_k \end{aligned} \tag{3.15}$$

where

$$E_k = \frac{\psi_k\|Q(w_k)-\tilde{o}\|^2 + 2(1-\psi_k)\langle Q(\tilde{o})-\tilde{o},\ \ S(w_k)-\tilde{o}\rangle + d_k\|Q(\tilde{o})-\tilde{o}\| + \frac{2d_k}{\psi_k}\|x_k-\tilde{o}\|}{1-\theta^2}.$$

There are two feasible cases:

Case I: If $\{\|w_k-\tilde{o}\|\}$ is monotonically decreasing, which guarantees the existence of a number N_1 such that $\|w_{k+1}-\tilde{o}\| \le \|w_k-\tilde{o}\|$ for all $k \ge N_1$. Hence, boundedness of $\{\|w_k-\tilde{o}\|\}$ implies that $\{\|w_k-\tilde{o}\|\}$ is convergent. Therefore, using (3.15), we have

$$\begin{aligned} 2\mu_k\kappa\Big\|Bu_k \quad &- \quad B\tilde{o} - \frac{u_k-v_k}{2\kappa}\Big\|^2 + \Big(\frac{2\kappa-\mu_k}{2\kappa}\Big)\|u_k-v_k\|^2 \\ &\le \quad \|w_k-\tilde{o}\|^2 - \|w_{k+1}-\tilde{o}\|^2 - \gamma_k\|w_k-\tilde{o}\|^2 + \gamma_k E_k. \end{aligned} \tag{3.16}$$

By taking limit $k\to\infty$, we get

$$\lim_{k\to\infty}\|u_k-v_k\| = 0. \tag{3.17}$$

From (3.3), (3.4), and using nonexpansive property of $R^G_{\mu_k}(I-\mu_k B)$, we infer that

$$\lim_{k\to\infty}\|w_{k+1}-v_k\| = 0. \tag{3.18}$$

Using (3.17) and (3.18), we get

$$\lim_{k\to\infty}\|w_{k+1}-u_k\| = 0. \tag{3.19}$$

From (3.4) and again using nonexpansive property of $R^G_{\mu_k}(I-\mu_k B)$, we get

$$\|w_{k+1}-w_k\| \le \|v_k-v_{k-1}\| \le \|u_k-u_{k-1}\|. \tag{3.20}$$

We also have

$$\begin{aligned} &\|x_k-x_{k-1}\| = \|Sw_k + \sigma_k(w_k-w_{k-1}) - Sw_{k-1} - \sigma_{k-1}(w_{k-1}-w_{k-2})\| \\ \le\ & \|w_k-w_{k-1}\| + \sigma_k\|w_k-w_{k-1}\| + \sigma_{k-1}\|w_{k-1}-w_{k-2}\| \\ \le\ & \|u_{k-1}-u_{k-2}\| + \sigma_k\|w_k-w_{k-1}\| + \sigma_{k-1}\|w_{k-1}-w_{k-2}\|. \end{aligned} \tag{3.21}$$

Since h is a contraction, $\{w_k\}$ and $\{x_k\}$ are bounded. Then, it results from (3.2), (3.20), and (3.21) that

$$\begin{aligned} &\|u_k-u_{k-1}\| = \|\psi_k Q(w_k) + (1-\psi_k)x_k - \psi_{k-1}Q(w_{k-1}) - (1-\psi_{k-1})x_{k-1}\| \\ =\ & \|\psi_k Q(w_k) - \psi_k Q(w_{k-1}) + \psi_k Q(w_{k-1}) + (1-\psi_k)x_k - (1-\psi_k)x_{k-1} \\ & +(1-\psi_k)x_{k-1} - \psi_{k-1}Q(w_{k-1}) - (1-\psi_{k-1})x_{k-1}\| \\ \le\ & \psi_k\theta\|w_k-w_{k-1}\| + |\psi_k-\psi_{k-1}|\{\|Q(w_{k-1})\| + \|\|x_{k-1}\|\} \\ & +(1-\psi_k)\|x_k-x_{k-1}\| \\ \le\ & \psi_k\theta\|u_{k-1}-u_{k-2}\| + (1-\psi_k)\|x_k-x_{k-1}\| + |\psi_k-\psi_{k-1}| \times L_2 \\ \le\ & \psi_k\theta\|u_{k-1}-u_{k-2}\| + (1-\psi_k)\{\|u_{k-1}-u_{k-2}\| + \sigma_k\|w_k-w_{k-1}\| \end{aligned}$$

$$
\begin{aligned}
&+\sigma_{k-1}\|w_{k-1}-w_{k-2}\|\}+|\psi_k-\psi_{k-1}|\times L_2\\
\leq\ &[1-\psi_k(1-\theta)]\|u_{k-1}-u_{k-2}\|+\sigma_k\|w_k-w_{k-1}\|+\sigma_{k-1}\|w_{k-1}-w_{k-2}\|\\
&+|\psi_k-\psi_{k-1}|\times L_2
\end{aligned}
$$

or

$$\|u_k-u_{k-1}\| \leq (1-a_k)\|u_{k-1}-u_{k-2}\|+b_k$$

where $a_k=\psi_k(1-\theta)$ and $b_k=\sigma_k\|w_k-w_{k-1}\|+\sigma_{k-1}\|w_{k-1}-w_{n-2}\|+|\psi_k-\psi_{k-1}|\times L_2$. It can be easily seen that $\sum_{k=1}^{\infty} a_k=\infty$ and $\sum_{k=1}^{\infty}|b_k|<\infty$. In the light of Lemma 2.3, we deduce that

$$\lim_{k\to\infty}\|u_k-u_{k-1}\|=0. \tag{3.22}$$

Hence

$$\lim_{k\to\infty}\|w_{k+1}-w_k\|=0. \tag{3.23}$$

It follows from (3.2) that

$$
\begin{aligned}
u_k-w_k &= \psi_kQ(w_k)+(1-\psi_k)x_k-w_k\\
&= \psi_k[Q(w_k)-w_k]+(1-\psi_k)(x_k-w_k)
\end{aligned}
$$

or

$$(1-\psi_k)\|x_k-w_k\| \leq \psi_k\|Q(w_k)-w_k\|+\|w_{k+1}-w_k\|+\|w_{k+1}-u_k\|.$$

Since $\psi_k\to 0$ as $k\to\infty$ and using (3.19) and (3.23), we get

$$\lim_{k\to\infty}\|x_k-w_k\|=0. \tag{3.24}$$

Since the sequence $\{w_k\}$ and $\{x_k\}$ are bounded and Q is a θ-contraction, it follows that

$$
\begin{aligned}
\|u_k-x_k\| &= \|\psi_kQ(w_k)-\psi_kx_k\|\\
&= \psi_k\|Q(w_k)-Q(\tilde{o})+Q(\tilde{o})-x_k\|\\
&\leq \psi_k[\theta\|w_k-\tilde{o}\|+\|Q(\tilde{o})-x_k\|]\\
&\leq \psi_k[\theta L_2+L_3],
\end{aligned}
$$

hence,

$$\lim_{k\to\infty}\|u_k-x_k\|=0. \tag{3.25}$$

From (3.2), we have

$$
\begin{aligned}
u_k &= \psi_kQ(w_k)+(1-\psi_k)[Sw_k+\sigma_k(w_k-w_{k-1})]\\
&= \psi_kQ(w_k)+Sw_k+\sigma_k(w_k-w_{k-1})-\psi_kx_k
\end{aligned}
$$

$$\begin{aligned} &= \psi_k[Q(w_k) - Q(\tilde{o})] + \sigma_k(w_k - w_{k-1}) + \psi_k[Q(\tilde{o}) - x_k] + Sw_k \\ \|u_k - Sw_k\| &\leq \psi_k\theta\|w_k - \tilde{o}\| + \sigma_k\|w_k - w_{k-1}\| + \psi_k\|Q(\tilde{o}) - x_k\| \\ &\leq \psi_k[\theta L_2 + L_3] + \sigma_k\|w_k - w_{k-1}\|. \end{aligned}$$

By taking limit $k \to \infty$, we obtain

$$\lim_{k\to\infty} \|u_k - Sw_k\| = 0. \tag{3.26}$$

Now, by using (3.24)–(3.26), we obtain

$$\|Sw_k - w_k\| \leq \|Sw_k - u_k\| + \|u_k - x_k\| + \|x_k - w_k\| \to 0 \text{ as } k \to \infty. \tag{3.27}$$

Boundedness of $\{w_k\}$ guarantees the existence of a subsequence $\{w_{k_m}\}$ converging weakly to $\overline{\omega}$. It follows from (3.18) and (3.19) that $\{u_{k_m}\}$ and $\{v_{k_m}\}$ also converge weakly to $\overline{\omega}$. By (3.3), we have

$$\frac{u_{k_m} - v_{k_m}}{\mu_k} - (Bu_{k_m} - Bv_{k_m}) \in (B + G)(v_{k_m}). \tag{3.28}$$

Let $(p, q) \in graph(B + G)$. By using monotonicity of $B + G$, we have

$$\left\langle q - \frac{u_{k_m} - v_{k_m}}{\mu_{k_m}} + (Bu_{k_m} - Bv_{k_m}), p - v_{k_m} \right\rangle \geq 0$$

or

$$\begin{aligned} \langle q, p - v_{k_m} \rangle &\geq \left\langle \frac{u_{k_m} - v_{k_m}}{\mu_{k_m}} - (Bu_{k_m} - Bv_{k_m}), p - v_{k_m} \right\rangle \\ &\geq \frac{1}{\mu}\langle u_{k_m} - v_{k_m}, p - v_{k_m} \rangle + \langle Bu_{k_m} - Bv_{k_m}, p - v_{k_m} \rangle. \end{aligned}$$

By taking limit $k \to \infty$, we get

$$\langle q, p - \overline{\omega} \rangle \geq 0$$

and maximal monotonicity of $B + G$ suggests that $0 \in (B + G)\overline{\omega}$, which means $\overline{\omega} \in \Phi$. Implementing Lemma 2.2 to (3.27), we infer that $\overline{\omega} \in Fix(S)$. Thus, $\overline{\omega} \in \Phi \cap \Omega$.

To conclude, we drive the strong convergence of the sequence $\{w_k\}$. From (3.15), we have

$$\|w_{k+1} - \tilde{o}\|^2 \leq (1 - \gamma_k)\|w_k - \tilde{o}\|^2 + \gamma_k E_k. \tag{3.29}$$

Furthermore,

$$\begin{aligned} &\limsup_{k\to\infty} E_k \\ &= \limsup_{k\to\infty} \frac{\psi_k\|Q(w_k) - \tilde{o}\|^2 + 2(1 - \psi_k)\left\langle Q(\tilde{o}) - \tilde{o},\ S(w_k) - \tilde{o} \right\rangle + d_k\|Q(\tilde{o}) - \tilde{o}\| + \frac{2d_k}{\psi_k}\|x_k - \tilde{o}\|}{1 - \theta^2} \\ &= \limsup_{m\to\infty} \frac{\psi_{k_m}\|Q(w_{k_m}) - \tilde{o}\|^2 + 2(1 - \psi_{k_m})\left\langle Q(\tilde{o}) - \tilde{o},\ S(w_{k_m}) - \tilde{o} \right\rangle + d_{k_m}\|Q(\tilde{o}) - \tilde{o}\| + \frac{2d_{k_m}}{\psi_{k_m}}\|x_{k_m} - \tilde{o}\|}{1 - \theta^2} \end{aligned}$$

$$= \langle Q(\tilde{o}) - \tilde{o}, \ \ \overline{\omega} - \tilde{o}\rangle$$
$$\leq 0.$$

Now we are in position to apply Lemma 2.3 in (3.29) and conclude that $\{w_k\}$ converges strongly to $\tilde{o}$. Hence, the result is proved.
Case II: If Case I is not true, then $\mathfrak{I} : \mathbb{N} :\to \mathbb{N}$ for all $k \geq k_0$ defined by $\mathfrak{I}(k) = \max\{m \in \mathbb{N} : k \geq m : \|w_k - \tilde{o}\| \leq \|w_{k+1} - \tilde{o}\|\}$ is increasing and $\lim_{k\to\infty} \mathfrak{I}(k) \to \infty$ and

$$0 \leq \|w_{\mathfrak{I}(k)} - \tilde{o}\| \leq \|w_{\mathfrak{I}(k)+1} - \tilde{o}\|, \ \forall \ k \geq k_0.$$

By using (3.15), we have

$$\begin{aligned} 2\mu_{\mathfrak{I}(k)}\kappa\Big\|Bu_{\Upsilon(k)} - B\tilde{o} + \frac{u_{\mathfrak{I}(k)} - v_{\mathfrak{I}(k)}}{2\kappa}\Big\|^2 \quad &+ \quad \Big(\frac{2\kappa - \mu_{\mathfrak{I}(k)}}{2\kappa}\Big)\|u_{\mathfrak{I}(k)} - v_{\mathfrak{I}(k)}\|^2 \\ &\leq \quad \gamma_{\mathfrak{I}(k)}E_{\mathfrak{I}(k)} - \gamma_{\mathfrak{I}(k)}\|w_{\mathfrak{I}(k)} - \tilde{o}\|^2. \end{aligned}$$

By taking limit $k \to \infty$, we get

$$\|u_{\mathfrak{I}(k)} - v_{\mathfrak{I}(k)}\| \to 0. \tag{3.30}$$

Following the similar steps used in the justification of Case I, we arrive at $\|w_{\mathfrak{I}(k)+1} - u_{\mathfrak{I}(k)}\| \to 0$ and $\|w_{\mathfrak{I}(k)+1} - v_{\mathfrak{I}(k)}\| \to 0$ as $k \to \infty$. From (3.29) and (3.30), we get

$$0 \leq \|w_{\mathfrak{I}(k)} - \tilde{o}\| \leq E_{\mathfrak{I}(k)}.$$

By taking limit $k \to \infty$ and using Lemma 2.5,

$$0 \leq \|w_k - \tilde{o}\| \leq \max\{\|w_k - \tilde{o}\|, \|w_{\mathfrak{I}(k)} - \tilde{o}\|\} \leq \|w_{\mathfrak{I}(k)+1} - \tilde{o}\|.$$

It follows that $\|w_k - \tilde{o}\| \to 0$ as $k \to \infty$. This establishes the result. □

Algorithm 3.2. Hybrid inertial iterative method 2

Choose $\sigma \in [0, 1)$, and $0 < \mu < \mu_k < 2\kappa$ is given. Pick the initial points w_0 and w_1.
Iterative Step: For $k \geq 1$ and iterates w_k, w_{k-1}, select $0 < \sigma_k < \overline{\sigma}_k$, where

$$\overline{\sigma}_k = \begin{cases} \min\{\frac{\tau_k}{\|w_k - w_{k-1}\|}, \quad \sigma\}, & \text{if } w_k \neq w_{k-1}, \\ \sigma, & \text{otherwise.} \end{cases}$$

Compute

$$u_k = \psi_k Q(w_k) + (1 - \psi_k)[w_k + \sigma_k(w_k - w_{k-1})], \tag{3.31}$$
$$v_k = R^G_{\mu_k}(u_k - \mu_k Bu_k) \tag{3.32}$$
$$w_{k+1} = SR^G_{\mu_k}(v_k - \mu_k Bv_k) \tag{3.33}$$

If $w_{k+1} = v_k = w_k = u_k$ then exit, or else, assign $k = k + 1$ and back to the computation.

Theorem 3.2. *If the assumptions* (A_1)–(A_5) *hold, then the sequence* $\{w_k\}$ *generated by Algorithm 3.2 converges strongly to w, where* $w = P_{\Phi\cap\Omega}Q(w)$.

Proof. Take $\tilde{o} \in \Phi \cap \Omega$, and replacing S by identity operator I in (3.11), we get that $\{u_k\}, \{v_k\}$, and $\{w_k\}$ are bounded. Denote $s_k = w_k + \sigma_k(w_k - w_{k-1})$, then using the similar steps as in (3.14), we get

$$\begin{aligned} \|u_k - \tilde{o}\|^2 \leq\ & [1 - \psi_k(1 - \theta_k^2)]\|w_k - \tilde{o}\|^2\| + \psi_k\Big\{\psi_k\|Q(w_k) - \tilde{o}\|^2 \\ & +2(1 - \psi_k)\langle Q(\tilde{o}) - \tilde{o},\ \ w_k - \tilde{o}\rangle + d_k\|Q(\tilde{o}) - \tilde{o}\| \\ & +\frac{2d_k}{\psi_k}\|y_k - \tilde{o}\|\Big\} \end{aligned} \tag{3.34}$$

where $d_k = \sigma_k\|w_k - w_{k-1}\|$. Denote $z_k = R^G_{\mu_k}(I - \mu_k B)v_k$, then from (3.33) and using the same steps used in (3.7), it can be concluded that

$$\begin{aligned} \|z_k - \tilde{o}\|^2 \leq\ & \|v_k - \tilde{o}\|^2 - 2\mu_k\kappa\Big\|Bv_k - B\tilde{o} - \frac{v_k - z_k}{2\kappa}\Big\|^2 \\ & -\Big(\frac{2\kappa - \mu_k}{2\kappa}\Big)\|v_k - z_k\|^2. \end{aligned} \tag{3.35}$$

In view of (3.7), (3.14), (3.34), and (3.35), we find

$$\begin{aligned} & \|w_{k+1} - \tilde{o}\|^2 \leq \|S z_k - \tilde{o}\|^2 \leq \|z_k - \tilde{o}\|^2 \\ \leq\ & (1 - \gamma_k)\|w_k - \tilde{o}\|^2 + \gamma_k E_k - 2\mu_k\kappa\Big\|Bu_k - B\tilde{o} - \frac{u_k - v_k}{2\kappa}\Big\|^2 \\ & -\Big(\frac{2\kappa - \mu_k}{2\kappa}\Big)\|u_k - v_k\|^2 - 2\mu_k\kappa\Big\|Bv_k - B\tilde{o} - \frac{v_k - z_k}{2\kappa}\Big\|^2 \\ & -\Big(\frac{2\kappa - \mu_k}{2\kappa}\Big)\|v_k - z_k\|^2, \end{aligned} \tag{3.36}$$

where

$$\begin{aligned} E_k &= \frac{\psi_k\|Q(w_k) - \tilde{o}\|^2 + 2(1 - \psi_k)\langle Q(\tilde{o}) - \tilde{o},\ \ w_k - \tilde{o}\rangle + d_k\|Q(\tilde{o}) - \tilde{o}\| + \frac{2d_k}{\psi_k}\|y_k - \tilde{o}\|}{1 - \theta^2}, \\ \gamma_k &= \psi_k(1 - \theta^2). \end{aligned}$$

Considering the Case(I) as in the derivation of Theorem 3.1, we achieve

$$\|u_k - v_k\| \to 0,\ \ \|v_k - z_k\| \to 0,\ \ n \to \infty. \tag{3.37}$$

In view of (3.20), (3.21), and replacing $S = I$ in (3.22), we get

$$\|w_{k+1} - w_k\| \leq \|v_k - v_{k-1}\| \leq \|u_k - u_{k-1}\| \to 0 \ \text{ as } k \to \infty. \tag{3.38}$$

Since $s_k = w_k + \sigma_k(w_k - w_{k-1})$, which implies that $\|s_k - w_k\| \leq \sigma_k\|w_k - w_{k-1}\| \to 0$ as $k \to \infty$, and using boundedness of $\{w_k\}$ and $\{s_k\}$, we get, by taking limit $k \to \infty$,

$$\begin{aligned} \|u_k - s_k\| &\leq \psi_k\|Q(w_k) - \tilde{o}\| + \psi_k\|\tilde{o} - s_k\| \\ &\leq \psi_k\{\theta\|w_k - \tilde{o}\| + \|\tilde{o} - s_k\|\} \end{aligned}$$

$$\leq \quad \psi_k\{\theta L_2 + L_3\} \to 0. \tag{3.39}$$

Employing (3.37)–(3.39), by taking $k \to \infty$, we get

$$\begin{aligned} &\|S z_k - z_k\| = \|w_{k+1} - z_k\| \\ \leq \quad &\|w_{k+1} - w_k\| + \|w_k - s_k\| + \|s_k - u_k\| + \|u_k - v_k\| + \|v_k - z_k\| \to 0. \end{aligned}$$

Since $\overline{\omega} \in \omega_w(w_k)$ and $\{w_k\}$ is bounded, which guarantees the existence of subsequence w_{k_m} and $w_{k_m} \rightharpoonup \overline{\omega}$ and so is the sequence $\{z_{k_m}\}$. Thus, applying Lemma 2.3, we obtain $\overline{\omega} \in \Omega$. The remaining of the proof can be completed by proceeding the same steps as in the proof of Theorem 3.1.

Some special cases of Algorithms 3.1 and 3.2 are given below for some arbitrary $z \in \mathbb{H}$.

Algorithm 3.3. A special instance of Algorithm 3.1

Choose $\sigma \in [0, 1)$, and $0 < \mu < \mu_k < 2\kappa$ is given. Pick initial points w_0 and w_1, any for $z \in \mathbb{H}$.
Iterative step: For $k \geq 1$ and iterates w_k, w_{k-1}, select $0 < \sigma_k < \overline{\sigma}_k$, where

$$\overline{\sigma}_k = \begin{cases} \min\{\frac{\tau_k}{\|w_k - w_{k-1}\|}, \quad \sigma\}, & \text{if } w_k \neq w_{k-1}, \\ \sigma, & \text{otherwise.} \end{cases}$$

Compute

$$\begin{aligned} u_k &= \psi_k z + (1 - \psi_k)[S(w_k) + \sigma_k(w_k - w_{k-1})], \\ v_k &= R^G_{\mu_k}(u_k - \mu_k B u_k), \\ w_{k+1} &= R^G_{\mu_k}(v_k - \mu_k B v_k). \end{aligned}$$

If $w_{k+1} = v_k = w_k = u_k$ then exit, or else, assign $k = k + 1$ and back to the computation.

Corollary 3.1. *Suppose that the assumptions* (A_1)–(A_5) *are valid. If* $\{w_k\}$ *is induced by Algorithm 3.3 then,* $w_k \to z = P_{\Phi\cap\Omega}(z)$.

Proof. Put $Q(w) = z$ in Algorithm 3.1, and following the corresponding steps used in the validation of Theorem 3.1, we establish the proof.

Algorithm 3.4. A special instance of Algorithm 3.2

Choose $\sigma \in [0,1)$, $0 < \mu < \mu_k < 2\kappa$. Pick any points w_0, w_1, for any $z \in \mathbb{H}$.
Iterative step: For $k \geq 1$ and iterates w_k w_{k-1}, select $0 < \sigma_k < \overline{\sigma}_k$, where

$$\overline{\sigma}_k = \begin{cases} \min\{\frac{\tau_k}{\|w_k - w_{k-1}\|}, \quad \sigma\}, & \text{if } w_k \neq w_{k-1}, \\ \sigma, & \text{otherwise.} \end{cases}$$

Compute

$$\begin{aligned} u_k &= \psi_k z + (1-\psi_k)[w_k + \sigma_k(w_k - w_{k-1})], \\ v_k &= R^G_{\mu_k}(u_k - \mu_k B u_k), \\ w_{k+1} &= S R^G_{\mu_k}(v_k - \mu_k B v_k). \end{aligned}$$

If $w_{k+1} = v_k = w_k = u_k$ then stop, if not, fix $k = k+1$ and back to the computation.

Corollary 3.2. *If the assumptions* (A_1) *and* (A_2) *are valid and* $\{w_k\}$ *is induced by Algorithm 3.4 then,* $w_k \to z = P_{\Phi\cap\Omega}(z)$.

Proof. Put z in place of $Q(w)$ in Algorithm 3.2, and following the corresponding steps used in the validation of Theorem 3.2, we establish the proof. □

4. Applications

Some theoretical applications of proposed algorithms are discussed below for solving the variational inequality and the convex minimization problem in conjunction with the fixed point problem.

4.1. The variational inequality problem

The variational inequality problem $\mathrm{VI_{nequality}P}$ for the operator $B : \mathbb{H} \to \mathbb{H}$ is to find $\tilde{o} \in \mathbb{D}$ such that

$$\langle B\tilde{o}, w - \tilde{o}\rangle \geq 0 \ \ \forall\, w \in \mathbb{D},$$

where B is $\frac{1}{\kappa}$-ism. Let Φ_1 be the solution set of the above defined $\mathrm{VI_{nequality}P}$. We know that solving $\mathrm{VI_{nequality}P}$ is a special case of solving $\mathrm{VI_{nclusion}P}$. In fact, the projection operator is the resolvent of the normal cone. Thus, the following outcomes are given below.

Algorithm 4.1. Choose $\sigma \in [0,1)$, and $0 < \mu < \mu_k < \frac{2}{\kappa}$ is given. Pick the initial points w_0 and w_1.

Iterative step: For $k \geq 1$ and iterates w_k, w_{k-1}, select $0 < \sigma_k < \overline{\sigma}_k$, where

$$\overline{\sigma}_k = \begin{cases} \min\{\frac{\tau_k}{\|w_k - w_{k-1}\|}, \quad \sigma\}, & \text{if } w_k \neq w_{k-1}, \\ \sigma, & \text{otherwise.} \end{cases}$$

Compute

$$\begin{aligned} u_k &= \psi_k Q(w_k) + (1-\psi_k)[S(w_k) + \sigma_k(w_k - w_{k-1})], \\ v_k &= \mathrm{P}_{\mathbb{D}}(u_k - \mu_k B u_k), \\ w_{k+1} &= \mathrm{P}_{\mathbb{D}}(v_k - \mu_k B v_k). \end{aligned}$$

If $w_{k+1} = v_k = w_k = u_k$ then, exit, or else, assign $k = k+1$ and back to the computation.

Theorem 4.1. *Let $B : \mathbb{H} \to \mathbb{H}$ be $\frac{1}{\kappa}$-ism and $S : \mathbb{D} \to \mathbb{D}$ is nonexpansive. Suppose that the assumptions $(A_3) - (A_5)$ hold and $\Phi_1 \cap \Omega \neq \emptyset$. If the sequence $\{w_k\}$ is produced by Algorithm 4.1, then $w_k \to w = P_{\Phi_1 \cap \Omega} Q(w)$.*

Algorithm 4.2. Choose $\sigma \in [0,1)$, and $0 < \mu < \mu_k < \frac{2}{\kappa}$ is given. Pick the initial points w_0 and w_1.

Iterative step: For $k \geq 1$ and iterates w_k, w_{k-1}, select $0 < \sigma_k < \overline{\sigma}_k$, where

$$\overline{\sigma}_k = \begin{cases} \min\{\frac{\tau_k}{\|w_k - w_{k-1}\|}, \quad \sigma\}, & \text{if } w_k \neq w_{k-1}, \\ \sigma, & \text{otherwise.} \end{cases}$$

Compute

$$\begin{aligned} u_k &= \psi_k Q(w_k) + (1-\psi_k)[w_k + \sigma_k(w_k - w_{k-1})], \\ v_k &= \mathrm{P}_{\mathbb{D}}(u_k - \mu_k B u_k), \\ w_{k+1} &= S\mathrm{P}_{\mathbb{D}}(v_k - \mu_k B v_k). \end{aligned}$$

If $w_{k+1} = v_k = w_k = u_k$ then exit, or else, assign $k = k+1$ and back to the computation.

Theorem 4.2. *Let $B : \mathbb{H} \to \mathbb{H}$ be $\frac{1}{\kappa}$-ism and $S : \mathbb{D} \to \mathbb{D}$ is nonexpansive. Suppose that the assumptions (A_3)–(A_5) hold and $\Phi_1 \cap \Omega \neq \emptyset$. If the sequence $\{w_k\}$ is induced by Algorithm 4.2, then $w_k \to w = P_{\Phi_1 \cap \Omega} Q(w)$.*

4.2. The convex optimization problem (CMP)

Let $V_1, V_2 : \mathbb{H} \to \mathbb{H}$ be two proper, convex and lower semi-continuous functions such that V_2 is differentiable and κ-Lipschitz continuous. The CMP for V_1 and V_2 is to find $\tilde{o} \in \mathbb{H}$ such that

$$V_1(\tilde{o}) + V_2(\tilde{o}) \leq V_1(w) + V_2(w), \quad \forall\, w \in \mathbb{H}.$$

Let the solution set of CMP be symbolized by Φ_2 . The CMP is equivalent to determining $w \in \mathbb{H}$ satisfying

$$0 \in \nabla V_1(\tilde{o}) + \partial V_2(\tilde{o})$$

where ∇V_1 is the gradient of V_1 and ∂V_2 is the subdifferential of V_2. We are aware of that every κ-Lipschitz continuous function is $\frac{1}{\kappa}$-ism and ∂V_2 is maximal monotone [34]. Thus, by replacing $B = \nabla V_1$ and $G = \partial V_2$ in Algorithms 3.1 and 3.2, the following consequences hold:

Algorithm 4.3. Choose $\sigma \in [0, 1)$, and $0 < \mu < \mu_k < \frac{2}{\kappa}$ is given. Pick the initial points w_0 and w_1.

Iterative step: For $k \geq 1$ and iterates w_k, w_{k-1}, select $0 < \sigma_k < \overline{\sigma}_k$, where

$$\overline{\sigma}_k = \begin{cases} \min\{\frac{\tau_k}{\|w_k - w_{k-1}\|}, \quad \sigma\}, & \text{if } w_k \neq w_{k-1}, \\ \sigma, & \text{otherwise.} \end{cases}$$

Compute

$$\begin{aligned} u_k &= \psi_k Q(w_k) + (1 - \psi_k)[S(w_k) + \sigma_k(w_k - w_{k-1})], \\ v_k &= R_{\mu_k}^{\partial V_2}(u_k - \mu_k \nabla V_1(u_k)), \\ w_{k+1} &= R_{\mu_k}^{\partial V_2}(v_k - \mu_k \nabla V_1(v_k)). \end{aligned}$$

If $w_{k+1} = v_k = w_k = u_k$, then exit, or else, assign $k = k + 1$ and return to the computation.

Theorem 4.3. *Let V_1 and V_2 be proper, convex, and lower semi-continuous functions such that ∇V_1 and ∂V_2 are maximal monotone and ∇V_1 is $\frac{1}{\kappa}$-ism. Suppose that the assumptions (A_3)–(A_5) hold and $\Phi_2 \cap \Omega \neq \emptyset$. Then, the sequence $\{w_k\}$ produced by Algorithm 4.3, converges strongly to w, where $w = P_{\Phi_2 \cap \Omega} Q(w)$.*

Algorithm 4.4. Choose $\sigma \in [0, 1)$, $0 < \mu < \mu_k < \frac{2}{\kappa}$ are given. Pick the initial points w_0 and w_1.

Iterative step: For $k \geq 1$ and iterates w_k, w_{k-1}, select $0 < \sigma_k < \overline{\sigma}_k$, where

$$\overline{\sigma}_k = \begin{cases} \min\{\frac{\tau_k}{\|w_k - w_{k-1}\|}, \quad \sigma\}, & \text{if } w_k \neq w_{k-1}, \\ \sigma, & \text{otherwise.} \end{cases}$$

Compute

$$\begin{aligned} u_k &= \psi_k Q(w_k) + (1 - \psi_k)[w_k + \sigma_k(w_k - w_{k-1})], \\ v_k &= R_{\mu_k}^{\partial V_2}(u_k - \mu_k \nabla V_1 u_k), \\ w_{k+1} &= S R_{\mu_k}^{\partial V_2}(v_k - \mu_k \nabla V_1 v_k). \end{aligned}$$

If $w_{k+1} = v_k = w_k = u_k$ then exit, or else, assign $k = k + 1$ and back to the computation.

Theorem 4.4. *Let $\mathbb{H}$ be a real Hilbert space and V_1 and V_2 be proper, convex and lower semi-continuous function such that ∇V_1 and ∂V_2 are maximal monotone and ∇V_1 is $\frac{1}{\kappa}$-ism. Suppose that the assumptions (A_3)–(A_5) hold and $\Phi_2 \cap \Omega \neq \emptyset$. Then the sequence $\{w_k\}$ produced by the Algorithm 4.4 converges strongly to w, where $w = P_{\Phi_2 \cap \Omega} Q(w)$.*

4.3. Image restoration problem

We are considering the following mathematical model for image restoration (or deblurring) problem:

$$y = Aw + \varepsilon,$$

where $y \in \mathbb{R}^N$ is assumed to be a blurred and noisy version of the original image $w \in \mathbb{R}^N$, where $A \in \mathbb{R}^{N\times N}$ represents the linear blur operator and ε is an additive noise term. Recovering the clean image is often formulated as the convex minimization problem

$$\min_{w\in\mathbb{R}^N} \Big\{F(w) := \tfrac{1}{2}\|Aw - y\|^2 + \lambda\,\Phi(w)\Big\},$$

where Φ is a regularization function and $\lambda > 0$ is a regularization parameter. The optimality condition of (4.1) can be expressed as the variational inclusion

$$0 \in A^\top(Aw - y) + \lambda\,\partial\Phi(w),$$

which fits the general inclusion form $0 \in B(w) + G(w)$ by setting

$$B(w) = A^\top(Aw - y), \qquad G(w) = \lambda\,\partial\Phi(w).$$

Hence, Algorithms 3.1 and 3.2 can be implemented to this imaging context.

The quality of the restored image is measured by the magnitude of the signal-to-noise ratio (SNR) in decibel (dB) and it is defined by:

$$\text{SNR} := 20\log_{10}\left(\frac{\|w\|_2}{\|\bar{w} - w\|_2}\right),$$

where w denotes the original image and $\bar{w}$ represents the restored (reconstructed) image. The PSNR (peak-signal-to-noise ratio) is a quantitative measure used to assess the quality of reconstructed or compressed images compared to their original versions. It is defined as

$$\text{PSNR} = 10\log_{10}\left(\frac{MAX_I^2}{MSE}\right)$$

where MAX_I=maximum possible pixel value (e.g., 1 for normalized images, 255 for 8-bit images), and MSE =mean squared error between the original and reconstructed images.

The first experiment is on the butterfly which we applied motion blur noise to the original image and restored it using the proposed Algorithms 3.1, 3.2 and 3 of [37]. The output is presented Figures 1, 2 and Table 1.

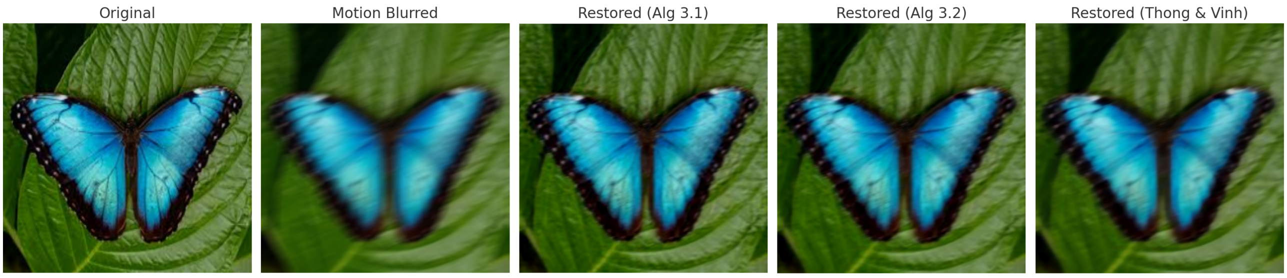

Figure 1. The image illustrates motion blur removal using three algorithms. The blurred butterfly image is gradually restored. Algorithm 3.1 produces sharper, more detailed reconstruction; Algorithm 3.2 offers smoother results; and the Algorithm 3 of [37] method balances sharpness with smoothness. Overall, Algorithm 3.1 yields the best clarity, effectively reversing motion blur while preserving visual fidelity.

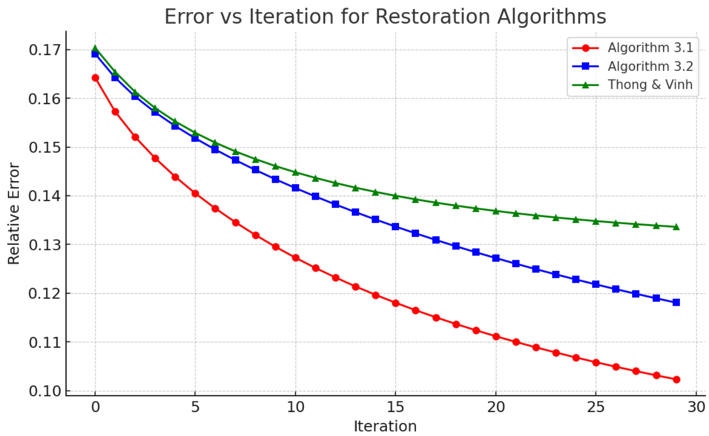

Figure 2. For the butterfly: Algorithm 3.1 demonstrates the fastest convergence with the lowest error, Algorithm 3.2 converges more gradually, while Algorithm 3 of [37] attains smoother yet slower convergence behavior.

Table 1. Performance comparison of the three image restoration algorithms using the butterfly image under motion blur. The table reports the SNR,PSNR, number of iterations, CPU (Central Processing Unit) running time, and algorithmic parameters (μ, λ, σ).

Algorithm	SNR (dB)	PSNR (dB)	Iterations	CPU Time (s)	μ	λ	σ
Algorithm 3.1	19.80	28.77	30	8.07	0.9	0.01	0.4
Algorithm 3.2	18.56	27.52	30	7.78	0.9	0.01	0.4
Algorithm 3 of [37]	17.48	26.45	30	11.76	0.9	0.01	0.4

We observe that Algorithm 3.1 achieved the best restoration quality with highest PSNR and SNR but required more time. Algorithm 3.2 was fastest, while Algorithm 3 of [37] produced smoother, more regularized but slightly blurred results.

Our second experiment is on a cameraman, blurred image with motion blur and restored with the three algorithms. The output is displayed below in Figures 3, 4 and Table 2.

Figure 3. The motion-blurred cameraman image was restored using three algorithms. Algorithm 3.1 achieved stronger sharpening but introduced slight artifacts. Algorithm 3.2 provided smoother yet slightly softer results. Algorithm 3 of [37] method produced a balanced restoration, preserving edges while reducing distortion. Overall, all methods effectively mitigated motion blur, with Algorithm 3 of [37] offering the best visual compromise.

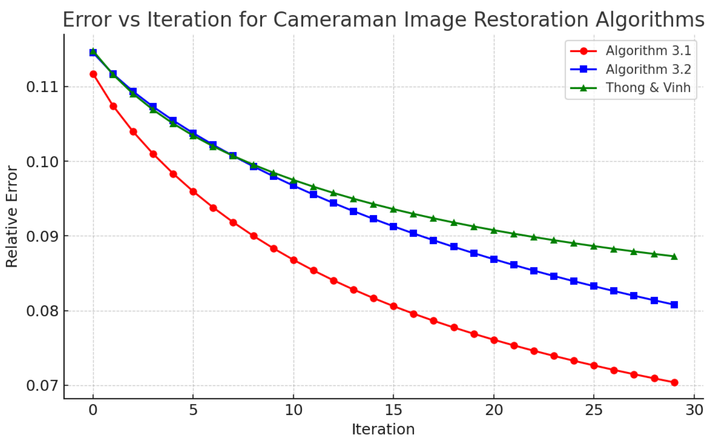

Figure 4. For the Cameraman: Algorithm 3.1 converges fastest with lowest error, Algorithm 3.2 stabilizes slower, while Algorithm 3 of [37] achieves smoother but slower convergence.

Table 2. Performance comparison of the three image restoration algorithms using the Cameraman image under motion blur. The table reports the signal-to-noise ratio SNR, PSNR, number of iterations, CPU running time, and algorithmic parameters (μ, λ, σ).

Algorithm	SNR (dB)	PSNR (dB)	Iterations	CPU Time (s)	μ	λ	σ
Algorithm 3.1	23.0512	27.7419	30	22.3708	0.9	0.005	0.4
Algorithm 3.2	21.8527	26.5435	30	11.5767	0.9	0.005	0.4
Algorithm 3 of [37]	21.1837	25.8744	30	16.5906	0.9	0.005	0.4

From Table 2, we notice that Algorithm 3.1 achieved the best restoration quality, yielding the highest SNR and PSNR with moderate computation time. Algorithm 3.2 performed slightly faster but with lower accuracy. Algorithm 3 of [37] produced smoother results but lower fidelity. Overall, Algorithm 3.1 balances accuracy and efficiency, making it the most effective reconstruction technique.

4.4. Transportation problem

Consider the classical transportation problem defined by a cost matrix $C = (c_{ij}) \in \mathbb{R}^{m\times n}$, supply vector $a = (a_1, \dots, a_m)$, and demand vector $b = (b_1, \dots, b_n)$ satisfying $\sum_{i=1}^{m} a_i = \sum_{j=1}^{n} b_j = 1$. The optimization model is

$$\begin{aligned} &\min_{X\in\mathbb{R}^{m\times n}} \quad \langle C, X\rangle \\ &\text{subject to} \quad X\mathbf{1}_n = a, \quad X^\top \mathbf{1}_m = b, \quad X \geq 0, \end{aligned} \tag{4.1}$$

where $X = (x_{ij})$ represents the transport plan. Let $A : \mathbb{R}^{m\times n} \to \mathbb{R}^{m+n}$ be the linear operator

$$A(X) = \begin{bmatrix} X\mathbf{1}_n \\ X^\top \mathbf{1}_m \end{bmatrix}, \quad d = \begin{bmatrix} a \\ b \end{bmatrix}.$$

The feasible set is $S = \{X \mid AX = d,\ X \geq 0\}$. Define the convex function $f(X) = \langle C, X\rangle$ and the normal cone operator $N_S(X)$ associated with S. Then, the optimality condition of (4.1) can be expressed as the following monotone inclusion problem:

$$0 \in \partial f(X) + N_S(X) = C + A^*\lambda + N_{\{X\geq 0\}}(X), \tag{4.2}$$

where A^* is the adjoint of A, and $\lambda \in \mathbb{R}^{m+n}$ is the vector of Lagrange multipliers for the equality constraints. Equation (4.2) defines a monotone inclusion problem, which can be solved using the iterative schemes developed for such operators.

To solve the inclusion (4.2), we apply Algorithms 3.1, 3.2 and 3 of [37] originally proposed for monotone inclusions and adapt it to the transportation problem. The iterative form employs inertial extrapolation and primal-dual updates.

Algorithm 4.5. (Algorithm 3.1 for Transportation Problem)

Input: cost $C \in \mathbb{R}^{m\times n}$, marginal a, b, initial $X_0 \geq 0$, dual λ_0, parameters $\tau > 0, \sigma > 0$, inertial weight $\alpha \in [0, \bar{\alpha})$, tolerance $\varepsilon > 0$. For $k = 0, 1, 2, \dots$
Inertial step: $Y_k = X_k + \alpha(X_k - X_{k-1}), \quad (Y_0 = X_0)$
Dual update: $\tilde{\lambda}_k = \lambda_k + \sigma(AY_k - d)$
Forward (gradient) step: $V_k = Y_k - \tau(C + A^*\tilde{\lambda}_k)$
Projection onto nonnegativity: $X_{k+1} = P_+(V_k) = \max(0, V_k)$
Dual correction:$\lambda_{k+1} = \tilde{\lambda}_k + \sigma(AX_{k+1} - AY_k)$
Stop: If $\|X_{k+1} - X_k\|_F / \max(1, \|X_k\|_F) < \varepsilon$ and $\|AX_{k+1} - d\| < \varepsilon$
Output: $X_{k+1}$is the approximate optimal transport plan.

The choice of parameters are listed in the Table 3.

Table 3. Parameter choice and remarks

Parameter / Remark	Description
Step sizes	Choose $\tau, \sigma > 0$ such that $\tau\sigma\|A\|^2 < 1$.
Bound on $\|A\|^2$	A practical bound is $\|A\|^2 \leq 2\max(m, n)$.
Inertial parameter	The inertial parameter satisfies $0 \leq \alpha < 1$, typically $\alpha = 0.2$.
Projection operator	The projection P_+ is elementwise and inexpensive to compute.
Computational complexity	Each iteration has $O(mn)$ computational complexity.

Algorithm 3.1 treats the transportation problem as a monotone inclusion by splitting the cost gradient, the affine constraints, and the nonnegativity cone. The dual variable λ enforces the marginal constraint.

Now, we present application of Algorithms 3.1, 3.2 and 3 of [37] to a transportation problem. Consider a transportation network consisting of three supply nodes and four demand nodes. The cost matrix C, supply vector a, and demand vector b are defined as follows:

$$C = \begin{bmatrix} 8 & 6 & 10 & 9 \\ 9 & 7 & 4 & 2 \\ 3 & 4 & 2 & 5 \end{bmatrix}, \quad a = (20, 15, 25), \quad b = (10, 25, 15, 10),$$

with $\sum_i a_i = \sum_j b_j = 60$. Algorithms 3.1, 3.2 and 3 of [37] were implemented using inertial parameter $\alpha = 0.2$, step sizes $\tau = \sigma = 0.1$, and tolerance $\varepsilon = 10^{-6}$. The algorithms were executed for up to 2000 iterations or until convergence. The results are presented and elaborated in Tables 4–6, Figures 5–7.

Table 4. Comparison of convergence and computational efficiency of the proposed algorithms with Algorithm 3 of [37]. Parameters: $\alpha = 0.2$, $\tau = \sigma = 0.1$, $\varepsilon = 10^{-6}$, dim = 50.

Method	Iterations	Final residual	Time (s)
Proposed Algorithm 3.1	287	9.34×10^{-7}	0.018
Proposed Algorithm 3.2	241	8.77×10^{-7}	0.015
Algorithm 3 of [37]	398	9.81×10^{-7}	0.024

Table 5. Objective convergence of proposed algorithms and Algorithm 3 of Thong & Vinh.

Iteration	Algorithm 3.1	Algorithm 3.2	Algorithm 3 of [37]
1	281.916667	306.166667	330.416667
2	230.250667	281.125167	–
3	189.549280	258.273151	–
4	165.351072	238.500665	–
5	156.587748	222.367467	–
6	158.926247	208.155992	–
7	167.485392	195.241256	–
8	179.275904	183.223756	–
9	191.786520	171.853964	–
10	203.240145	161.000233	–

Table 6. Final transportation plans $X = (x_{ij})$ obtained by the three algorithms.

Demand node	Algorithm 3.1			Algorithm 3.2			Thong & Vinh (2019)		
	S_1	S_2	S_3	S_1	S_2	S_3	S_1	S_2	S_3
D_1	0.000	0.000	10.012	0.000	0.000	10.055	3.333	2.500	4.167
D_2	19.975	0.000	5.044	19.970	0.000	5.083	8.333	6.250	10.417
D_3	0.000	5.056	9.936	0.000	5.084	9.888	5.000	3.750	6.250
D_4	0.000	9.968	0.000	0.000	9.970	0.000	3.333	2.500	4.167
Row sum	19.975	15.023	24.992	19.970	15.054	24.971	20.000	15.000	25.000
Column sum	10.012	25.019	14.991	10.055	25.032	14.987	10.000	25.000	15.000

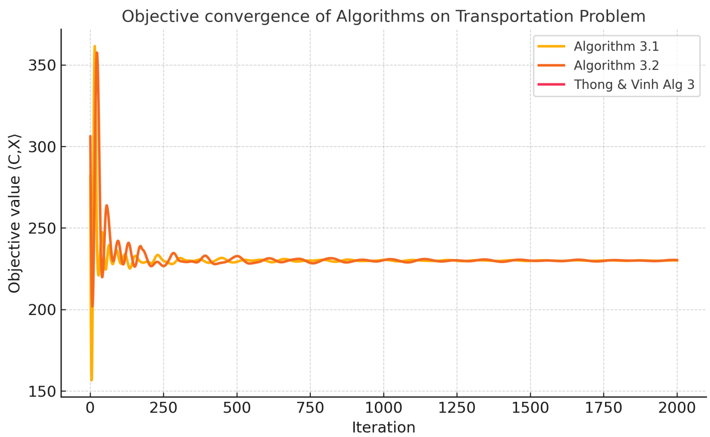

Figure 5. The graph shows that the Algorithm 3.1 decreases the cost fastest and stabilizes around 230, indicating better convergence. Algorithm 3.2 converges slowly with slightly higher final cost. Algorithm 3 of [37] remains flat, confirming it stayed at its initial feasible point without improvement.

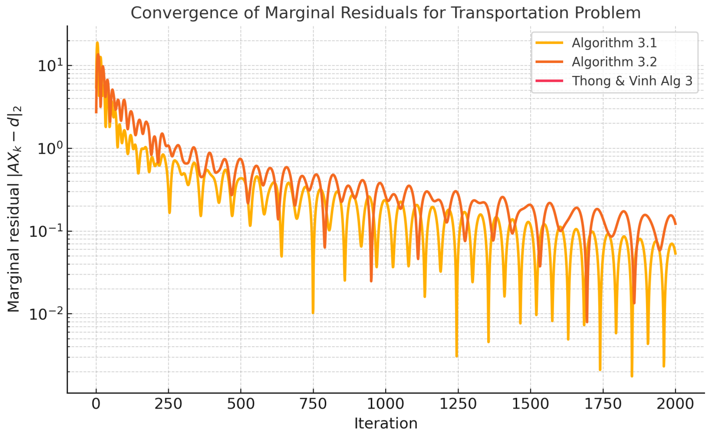

Figure 6. The plot illustrates how each algorithm reduces the marginal residual $\|AX_k - d\|_2$ over iterations. Algorithm 3.1 exhibits the fastest and most stable convergence toward feasibility. Algorithm 3.2 converges slowly, maintaining larger residuals. Algorithm 3 of [37] remains constant, indicating no improvement from an already feasible initial point.

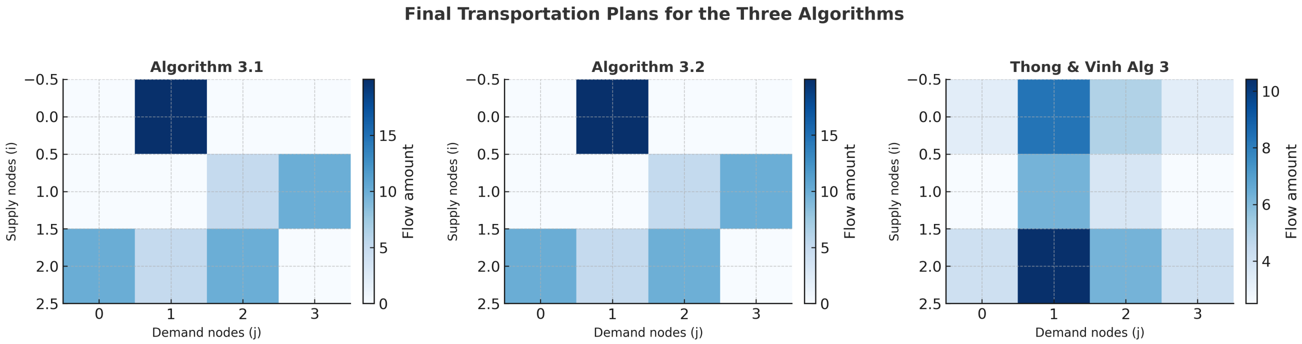

Figure 7. The color intensity in the hetmans represents the magnitude of transportation flows. Darker blue regions correspond to higher shipment volumes, while lighter shades indicate minimal or zero transport. Algorithm 3.1 shows concentrated dark areas along cost-efficient routes. Algorithm 3.2 exhibits similar but slightly diffused color patterns. The Algorithm 3 of [37] presents evenly distributed lighter tones, reflecting a more uniform but less cost-effective allocation.

From Table 4, it is observed that Proposed Algorithms 3.1 and 3.2 converge faster than Algorithm 3 of [37], requiring 241–287 vs. 398 iterations and 0.015–0.018 vs. 0.024 seconds, achieving residuals below 10^{-6} in dim = 50.

The Table 5 shows that the Algorithm 3.1 demonstrates a steady decline in objective values during early iterations, stabilizing faster than Algorithm 3.2. Algorithm 3.2 converges slowly, while Algorithm 3 of [37] lacks comparable data, suggesting delayed or incomplete convergence.

The Table 6 represents how goods are distributed from three supply centers (S_1–S_3) to four demand destinations (D_1–D_4). Each entry x_{ij} indicates the quantity of goods (in suitable units, e.g., tons or truckloads) shipped from supply node S_i to demand node D_j.

Under Algorithm 3.1, almost all of S_1's 20 units (about 99.9%) are delivered to D_2, suggesting this route is the most cost-effective. Supply node S_2 mainly serves D_3 and D_4, sending approximately 34% of its goods to D_3 and 66% to D_4. Meanwhile, S_3 supplies D_1–D_3, with around 40% to D_1, 20% to D_2, and 40% to D_3.

Algorithm 3.2 shows a very similar pattern but slightly less balanced, causing marginally higher residual errors in meeting the exact supply-demand requirements. For Algorithm 3 of [37], shipments are more evenly distributed: each supplier serves all four destinations in roughly proportional quantities. However, this uniform allocation results in a higher total cost, since it ignores the cost-optimal routing preferences revealed in the first two methods.

Overall, Algorithm 3.1 yields the most realistic and efficient logistics plan-minimizing transport cost while closely matching the supply and demand constraints. In practical terms, it would ensure timely deliveries with minimal empty returns or over-supply at any destination.

5. Numerical experiments

Example 5.1. (Finite dimensional) Let $\mathbb{H} = \mathbb{R}^2$. For $\zeta = (\zeta_1, \zeta_2)$ and $\upsilon = (\upsilon_1, \upsilon_2) \in \mathbb{R}^2$, the usual inner product, that is, $\langle \zeta, \upsilon \rangle = \zeta_1\upsilon_1 + \zeta_2\upsilon_2$ and $\|\zeta\|^2 = |\zeta_1|^2 + |\zeta_2|^2$. The operators B, G, and map S are defined by

$$B(\zeta_1, \zeta_2) = \Big(\frac{\zeta_1}{3}, \frac{\zeta_2}{5}\Big), \;\; G(\zeta_1, \zeta_2) = \Big(\frac{\zeta_1}{2}, \frac{\zeta_2}{3}\Big), \;\; S(\zeta_1, \zeta_2) = (\zeta_1, \zeta_2).$$

It is not hard to show that the operator B is 3-ism and $\frac{1}{5}$-strongly monotone, $\frac{1}{3}$-Lipschitz continuous; G is maximal monotone and S is nonexpansive.

For the computation, we choose $\psi_k = \frac{1}{\sqrt{k+1}}, \mu_k = \frac{5}{3} - \frac{1}{k+10}$, $\mu = \frac{3}{2}$, $\sigma = 0.4$, and σ_k is selected randomly from $(0, \bar{\sigma_k})$ where

$$\overline{\sigma}_k = \begin{cases} \min\{\frac{1}{(10+k)^3\|w_k - w_{k-1}\|}, & 0.4\}, \quad \text{if } w_k \neq w_{k-1}, \\ 0.4, & \text{otherwise} \end{cases}$$

We depict the convergence of sequences obtained from Algorithm 3 of [37], Algorithms 3.1–3.4. The algorithm terminates when $\|w_{k+1} - w_k\| < 10^{-16}$ for the succeeding initial values:
Case (a): $w_0 = (1, -8), \;\; w_1 = (-3, 5)$;
Case (b): $w_0 = (10, -18), \;\; w_1 = (53, 50)$;

It is evident that our algorithms are effective and can be simply executed. The convergence of $\{w_k\}$ to $\{0\} = \Phi \cap \Omega$ is shown in Figures 8 and 9 with varying values of contraction h. It is noted that our algorithms approach toward the solution in less steps in comparison to Algorithm 3 of [37].

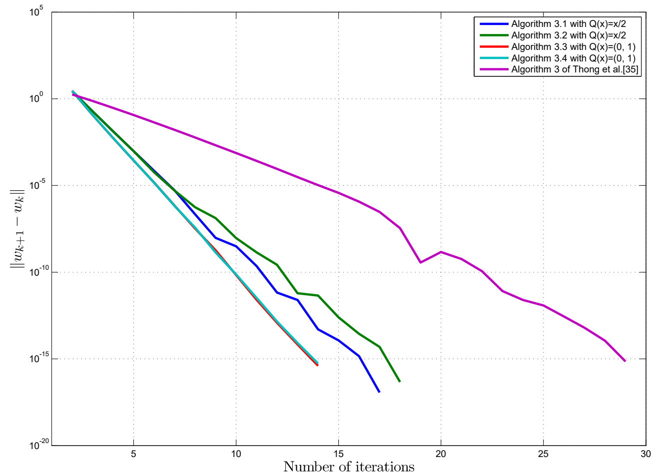

Figure 8. Pictorial presentation of $\|w_{k+1} - w_k\|$ induced by Algorithm 3 of [37], Algorithms 3.1–3.4 by using Case(a).

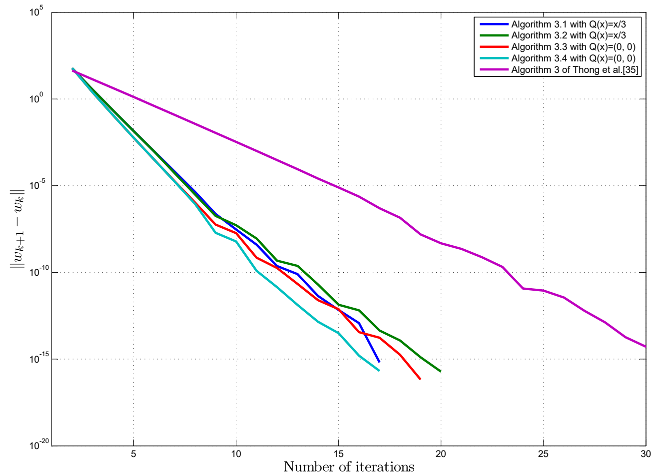

Figure 9. Pictorial presentation of $\|w_{k+1} - w_k\|$ induced by Algorithm 3 of [37], Algorithm 3.1–3.4 by using Case(b).

Example 5.2. (Infinite dimensional) Let $\mathbb{H} = l_2 := \{\vartheta := (\vartheta_1, \vartheta_2, \vartheta_3, \cdots, \vartheta_k, \cdots), \vartheta_k \in \mathbb{R} : \sum_{k=1}^{\infty} |\vartheta_k|^2 < \infty\}$, with inner product $\langle \vartheta, \upsilon \rangle = \sum_{n=1}^{\infty} \vartheta_k \upsilon_k$ and the norm $\|\vartheta\| = \Big(\sum_{k=1}^{\infty} |\vartheta_k|^2 \Big)^{1/2}$. The mappings B, G, and S are expressed by

$$B(\vartheta) := \frac{\vartheta}{5} \;\; G(\vartheta) := \frac{\vartheta}{3} \;\; S(\vartheta) := \vartheta, \quad \forall\, \vartheta \in l_2.$$

Clearly, B is 5-ism, G is maximal monotone, and S is nonexpansive. We choose $\mu_k = \frac{3}{2} - \frac{1}{k+20}$, $\mu = \frac{3}{2}$,

$\sigma = 0.3$, and σ_k is randomly selected from $(0, \overline{\sigma}_k)$, where

$$\overline{\sigma}_k = \begin{cases} \min\{\frac{1}{(k+10)^3\|w_k - w_{k-1}\|}, \quad 0.3\}, & \text{if } w_k \neq w_{k-1}, \\ 0.3, & \text{otherwise.} \end{cases}$$

We depict the convergence of the sequences produced by Algorithm 3 of [37], Algorithms 3.1–3.4. The algorithm terminates when $\|w_{k+1} - w_k\| < 10^{-15}$ for the succeeding two initial values:

Case (a'): $w_0 = \left\{\frac{(-1)^k}{k}\right\}_{k=1}^{\infty}$, $w_1 = \begin{cases} 0, & if\ k\ is\ odd, \\ \frac{1}{k^2}, & if\ k\ is\ even. \end{cases}$

Case (b'): $w_0 = \left\{\frac{1}{k}\right\}_{k=1}^{\infty}$, $w_1 = \left\{\frac{1}{k^2}\right\}_{k=1}^{\infty}$.

Our algorithms are implemented easily and found effective. We select different values of contraction h and visualize the convergence of $\{w_k\}$ to $\{0\} = \Phi \cap \Omega$ in Figures 10 and 11. It is noted that our algorithms converge in fewer steps in contrast to Algorithm 3 of [37].

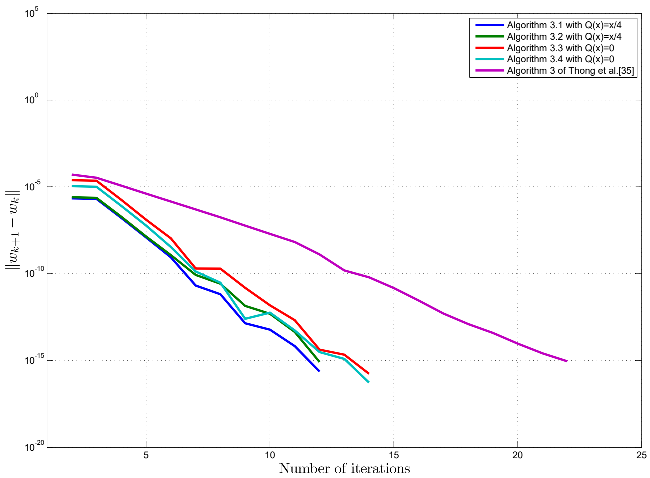

Figure 10. Pictorial presentation of $\|w_{k+1} - w_k\|$ induced by Algorithm 3 of [37], Algorithm 3.1–3.4 by using Case(a').

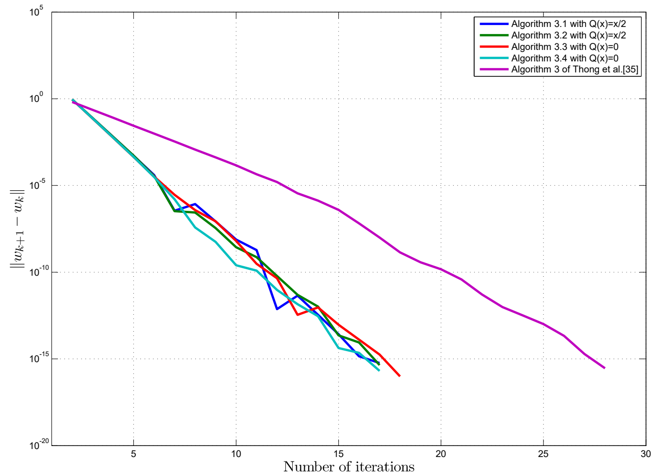

Figure 11. Pictorial presentation of $\|w_{k+1} - w_k\|$ induced by Algorithm 3 of [37], Algorithm 3.1–3.4 by using Case(b').

6. Conclusions

We have suggested two hybrid inertial viscosity-type forward-backward splitting iterative algorithms for solving $\mathrm{VI}_{\mathrm{nclusion}}\mathrm{P}$ and FPP in the environment of Hilbert spaces. We established the strong convergence of the sequences produced by the recommended methods in such a way that the iteration of the first algorithm begins with the computation of the viscosity iteration, fixed point iteration and inertial extrapolation while the second algorithm computes the viscosity and inertial extrapolation in the initial step of each iterations. Some special cases and some theoretical applications to solve variational inequality and convex optimization problems are discussed. We also studied the image restoration problem and transportation problem as advantages of our methods. Finally, we demonstrated the suggested approaches by using numerical experiments in the context of finite and infinite dimensional Hilbert spaces. Our methods can be implemented easily and approaches to the solution in less number of steps in contrast to the Algorithm 3 of [37].

It is worth mentioning that a comparative study on the convergence rate between the proposed method and other existing approaches for solving $\mathrm{VI}_{\mathrm{nclusion}}\mathrm{P}$ and FPP constitutes an interesting topic for future research.

Author contributions

D. Filali: Funding, supervision; M. Dilshad: writing–original draft preparation, writing–review and editing; M. Akram: Conceptualization; M. F. Khan: Review and editing; S. S. Irfan: Supervision. All authors have read and approved the final version of the manuscript for publication.

Use of Generative AI tools declaration

The authors declare they have not used AI tools in the creation of this article.

Acknowledgements

The first author acknowledges the Princess Nourah bint Abdulrahman University Researchers Supporting Project (Project Number PNURSP2025R174), Princess Nourah bint Abdulrahman University, Riyadh, Saudi Arabia.

Conflict of interest

The authors declare no conflicts of interest.

References

1. A. Alamer, M. Dilshad, Halpern-type inertial iteration methods with self-adaptive step size for split common null point problem, *Mathematics*, **12** (2024), 747. https://doi.org/10.3390/math12050747
2. T. O. Alakoya, O. J. Ogunsola, O. T. Mewomo, An inertial viscosity algorithm for solving monotone variational inclusion and common fixed point problems of strict pseudocontractions, *Bol. Soc. Mat. Mex.*, **29** (2023), 31. https://doi.org/10.1007/s40590-023-00502-6
3. M. Al-Qurashi, S. Rashid, F. Jarad, E. Ali, R. H. Egami, Dynamic prediction modelling and equilibrium stability of a fractional discrete biophysical neuron model, *Results Phys.*, **48** (2023), 106405. https://doi.org/10.1016/j.rinp.2023.106405
4. Y. Alber, I. Ryazantseva, Nonlinear Ill-posed problems of monotone type, Dordrecht: Springer, 2006. https://doi.org/10.1007/1-4020-4396-1
5. F. Alvarez, H. Attouch, An inertial proximal method for maximal monotone operators via discretization of a nonlinear osculattor with damping, *Set-Valued Anal.*, **9** (2001), 3–11. https://doi.org/10.1023/A:1011253113155
6. F. E. Browder, Nonlinear mapping of nonexpansive and accretive-type in Banach spaces, *Bull. Am. Math. Soc.*, **73** (1967), 875–882. https://doi.org/10.1090/S0002-9904-1967-11823-8
7. J. Y. Bello Cruz, R. Diaz Millan, A variant of forward-backward splitting method for the sum of two monotone operators with new search strategy, *Optimization*, **64** (2015), 1471–1486. https://doi.org/10.1080/02331934.2014.883510
8. H. H. Bauschke, P. L. *Combettes, convex analysis and monotone operator theory in Hilbert space*, Berlin: Springer, 2011. https://doi.org/10.1007/978-1-4419-9467-7
9. L. C. Ceng, Q. H. Ansari, M. M. Wong, J. C. Yao, Mann type hybrid extragradient method for variational inequalities, variational inclusions and fixed point problems, *Fixed Point Theor.*, **13** (2012), 403–422.
10. L. C. Ceng, Q. H. Ansari, J. C. Yao, Viscosity approximation methods for generalized equilibrium problems and fixed point problems, *J. Global Optim.*, **43** (2009), 487–502. https://doi.org/10.1007/s10898-008-9342-6
11. W. Cholamjiak, P. Cholamjiak, S. Suantai, An inertial forward-backward splitting method for solving inclusion problems in Hilbert spaces, *J. Fixed Point Theory Appl.*, **20** (2018), 42. https://doi.org/10.1007/s11784-018-0526-5

12. P. L. Combettes, V. R. Wajs, Signal recovery by proximal forward-backward splitting, *Multiscale Model. Simul.*, **4** (2005), 1168–1200. https://doi.org/10.1137/050626090

13. C. E. Chidume, Iterative construction of fixed points for multivalued operators of the monotone type, *Appl. Anal.*, **23** (1986), 209–218. https://doi.org/10.1080/00036818608839641

14. M. Dilshad, F. M. Alamrani, A. Alamer, E. Alshaban, M. G. Alshehri, Viscosity-type inertial iterative methods for variational inclusion and fixed point problems, *AIMS Math.*, **9** (2024), 18553–18573. https://doi.org/10.3934/math.2024903

15. M. Dilshad, M. Akram, M. Nsiruzzaman, D. Filali, A. A Khidir, Adaptive inertial Yosida approximation iterative algorithms for split variational inclusion and fixed point problems, *AIMS Math.*, **8** (2023), 12922–12942. https://doi.org/10.3934/math.2023651

16. V. H Dang, P. K. Anh, D. M. Le, Modified forward-backward splitting method for variational inclusions, *4OR-Q J. Oper. Res.*, **19** (2021), 127–151. https://doi.org/10.1007/s10288-020-00440-3

17. D. Filali, M. Dilshad, L. S. M. Alyasi, M. Akram, Inertial iterative algorithms for split variational inclusion and fixed point problems, *Axioms*, **12** (2023), 848. https://doi.org/10.3390/axioms12090848

18. F. Facchinei, J. S. Pang, *Finite-dimensional variational inequalities and complementarity problems*, New York: Springer, 2003. https://doi.org/10.1007/b97543

19. K. Geobel, W. A. Kirk, *Topics in metric fixed poit theory*, Cambridge University Press, 1990. https://doi.org/10.1017/CBO9780511526152

20. M. H. Heydari, S. Rashid, F. Jarad, A numerical method for distributed-order time fractional 2D Sobolev equation, *Results Phys.*, **45** (2023), 106211. https://doi.org/10.1016/j.rinp.2023.106211

21. D. Lorenz, T. Pock, An inertial forward-backward algorithm for monotone inclusions, *J. Math. Imaging Vis.*, **51** (2015), 311–325. https://doi.org/10.1007/s10851-014-0523-2

22. P. L. Lions, B. Mercier, Splitting algorithms for the sum of two nonlinear operators, *SIAM J. Numer. Anal.*, **16** (1979), 964–979. https://doi.org/10.1137/0716071

23. Y. Malitsky, M. K. Tam, A forward-backward splitting method for monotone inclusions without cocoercivity, *SIAM J. Optim.*, **30** (2020), 1451–1472. https://doi.org/10.1137/18M1207260

24. P. E. Mainge, Strong convergence of projected subgradient methods for nonsmooth and nonstrictly convex minimization, *Set-Valued Anal.*, **16** (2008), 899–912. https://doi.org/10.1007/s11228-008-0102-z

25. A. Moudafi, Split monotone variational inclusions, *J. Optim. Theory Appl.*, **150** (2011), 275-283. https://doi.org/10.1007/s10957-011-9814-6

26. A. Moudafi, M. Oliny, Convergence of a splitting inertial proximal method for monotone operators, *J. Comput. Appl. Math.*, **155** (2003), 447–454. https://doi.org/10.1016/S0377-0427(02)00906-8

27. A. Moudafi, Viscosity approximation methods for fixed-points problems, *J. Math. Anal. Appl.*, **241** (2000), 46–55. https://doi.org/10.1006/jmaa.1999.6615

28. W. Mann, Mean value methods in iteration, *Amer. Math. Soc.*, **4** (1953), 506-510. https://doi.org/10.2307/2032162

29. F. O. Nwawuru , O. K. Nrain, M. Dilshad, J. N. Ezeora, Splitting method involving two-step inertial for solving inclusion and fixed point problems with applications, *Fixed Point Theory Algorithms Sci. Eng.*, **2025** (2025), 8. https://doi.org/10.1186/s13663-025-00781-w

30. Z. Opial, Weak covergence of the sequence of successive approximations of nonexpansive mappings, *Bull. Amer. Math. Soc.*, **73** (1967), 591–597. https://doi.org/10.1090/S0002-9904-1967-11761-0

31. G. B. Passty, Ergodic convergence to a zero of the sum of monotone operators in Hilbert space, *J. Math. Anal. Appl.*, **72** (1979), 383–390. https://doi.org/10.1016/0022-247X(79)90234-8

32. S. Reich, A. Taiwo, Fast hybrid iterative schemes for solving variational inclusion problems, *Math. Method. Appl. Sci.*, **46** (2023), 17177–17198,. https://doi.org/10.1002/mma.9494

33. H. Raguet, J. Fadili, G. Peyre, A generalized forward-backward splitting, *SIAM J. Imaging Sci.*, **6** (2013), 1199–1226. https://doi.org/10.1137/120872802

34. R. T. Rockafellar, On the maximality of subdifferential mappings, *Pac. J. Math.*, **33** (1970), 209–216. https://doi.org/10.2140/PJM.1970.33.209

35. Y. Song, Iterative approximation to common fixed points of a countable family of nonexpansive mappings, *Appl. Anal.*, **86** (2007), 1329–1337. https://doi.org/10.1080/00036810701556144

36. A. Taiwo, O. T. Mewomo, A. Gibali, A simple strong convergent method for solving split common fixed point problems, *J. Nonlinear Var. Anal.*, **5** (2021), 777–793. https://doi.org/10.23952/jnva.5.2021.5.10

37. D. Thong, N. Vinh, Inertial methods for fixed point problems and zero point problems of the sum of two monotone mappings, *Optimization*, **68** (2019), 1037–1072. https://doi.org/10.1080/02331934.2019.1573240

38. P. Tseng, A modified forward-backward splitting method for maximal monotone mappings, *SIAM J. Control Optim.*, **38** (2000), 431–446. https://doi.org/10.1137/S0363012998338806

39. K. K. Tan, H. K. Xu, Approximating fixed points of nonexpansive mappings by the Ishikawa iteration process, *J. Math. Anal. Appl.*, **178** (1993), 301–308. https://doi.org/10.1006/jmaa.1993.1309

40. Y. Tang, H. Lin, A. Gibali, Y. J. Cho, Convegence analysis and applicatons of the inertial algorithm solving inclusion problems, *Appl. Numer. Math.*, **175** (2022), 1–17. https://doi.org/10.1016/j.apnum.2022.01.016

41. H. K. Xu, Another control condition in an iterative maethod for nonexpansive mappings, *Bull. Aust. Math. Soc.*, **65** (2002), 109–113. https://doi.org/10.1017/S0004972700020116

42. I. Yamada, The hybrid steepest descent method for the variational inequality problem over the intersection of fixed point sets of nonexpansive mappings, *Stud. Comput. Math.*, **8** (2001), 473–504. https://doi.org/10.1016/S1570-579X(01)80028-8